Electron Detachment from Negative Hydrogen Ions in Collisions with Neutral Atoms and Positive Ions at High Energies

TOSHIHIRO W IMAI

DOCTOR of SCIENCE

Department of Fusion Science
School of Mathematics and Physical Science
The Graduate University for Advanced Studies

1998

Abstract

High energy neutral hydrogen atom beam is used in the Neutral atom Beam Injection (NBI) for effective plasma heating in nuclear fusion research. There are two methods for production of neutral hydrogen atoms; one is electron capture process of positive hydrogen ions (protons) and the other is electron detachment process of negative hydrogen (H^-) ions. However, at high energies (more than 100 keV), the single electron detachment from H^- ions is much more efficient because the electron detachment cross sections from H^- ions are far larger than the electron capture cross sections of protons.

In the present thesis, we perform some theoretical analysis on the single electron detachment processes of H^- ions in collisions with neutral atoms and also with positive ions.

There are two electrons with different ionization potentials in a H^- ion in the ground state. We treat independently two electrons with different binding energies: one is the tightly bound 1s electron (ionization energy $\simeq$ 13.6 eV) and the other is the loosely bound 1s' electron (ionization energy $\simeq$ 0.75 eV) in the Hylleraas-Eckart function. Therefore, we take into account two different detachment processes, namely i) detachment of the tightly bound (1s) electron and ii) detachment of the loosely bound (1s') electron. To describe more detail of the electron detachment processes, the binding energies of each electron are taken into account in the detached electron wave functions. By these methods, we calculate the cross sections for production of hydrogen atoms not only in the ground state, $H^0(1s)$, but also in the excited states, $H^0(2s)$ and $H^0(2p)$, in the exit channel.

In collisions with neutral atoms including rare gases and atomic hydrogens, we use the first Born approximation to calculate the electron detachment

cross sections from H^- ions. we also consider the target excitation in the exit channel. However, as it is too much time-consuming to calculate all the possible states of target in the exit channel, we use the closure approximation for the target excitation.

First, we present the calculated results of the total and partial single-electron detachment cross sections from H^- ions in collisions with He and H neutral atoms. Then, we compare the calculated total cross sections of electron detachment with experimental data available and find reasonable agreement between them.

The calculated partial cross sections for the production the ground state hydrogen atoms, $H^0(1s)$, are found to be dominant in all the collision energy range (10 keV $\sim$ 10 MeV) investigated in the present study. The cross sections for $H^0(2s)$ formation are found to account for about 20 % and those for $H^0(2p)$ formation about 10 % of total electron detachment cross sections.

The present calculated results show that the dominant contribution to the production of the ground state $H^0(1s)$ comes from the electron detachment of the loosely bound 1s' electron in H^- ions. On the other hand, in the production of the excited state hydrogen atoms $H^0(2s)$ and $H^0(2p)$, the detachment of the tightly bound 1s electron in H^- ions is found to be dominant over the detachment of the loosely bound 1s' electron.

In collisions with positive ions, we use the Four-Body Continuum Distorted Wave-Eikonal Initial State (4-B CDW-EIS) method to calculate the electron detachment cross sections from H^- ions because there are strong distortion effects to its electrons due to the Coulomb field of the incident positive ions. Thus we consider the distorted waves and the distorted potentials. Though

the transition amplitudes are given in two different forms, namely the 'prior' and the 'post' because there are two distortion potentials, we treat the prior transition amplitudes only here.

Then, we compare the calculated total electron detachment cross sections from H^- ions in collisions with protons with experimental data.

We also notice that in general, in collisions with positive ions, the calculated partial cross sections of production of $H^0(1s)$ is far larger (more than two orders of magnitude) than those of $H^0(2s)$ in all the energies investigated.

The present calculated results also show that the total electron detachment cross sections of H^- ions in collisions with protons are roughly one order of magnitude greater than those with neutral hydrogen atoms and suggest a simple scaling which indicates that the electron detachment cross sections at high energies are roughly proportional to the square of the positive ion charge colliding with H^- ions.

These results suggest that H^- ions can be converted into neutral hydrogen atoms with more fraction of the ground state more efficiently in collisions with positive ions than in collisions with neutral atoms, indicating that in producing neutral hydrogen atoms for NBI from H^- ions the plasma neutralizer is indeed more promising than the neutral gas neutralizer which is widely used.

Contents

1 Introduction 1

2 Choice of wave functions 6

2.1 Wave function in the entrance channel 6

2.2 Wave function in the exit channel 7

3 Single electron detachment from H^- ions in collisions with neutral atoms (He and H) 9

3.1 Outline of present theory 9

3.2 Calculations 10

3.3 Results and discussion 17

3.3.1 Colliding with helium atoms 17

3.3.2 Colliding with hydrogen atoms 21

4 Single electron detachment from H^- ions in collisions with bare positive ions 39

4.1 Outline of present theory 39

4.2 Calculations 40

4.3 Results and discussion 47

5 Applications to NBI heating 59

5.1 Influence of present calculated results to NBI 59

6 Future problems 66

6.1 Double electron detachment 66

7 Conclusion **69**

Appendix 71

A The wave function for the detached electron **71**

B Distorted potential in the entrance channel **72**

C Distorted potential in the exit channel **74**

D Numerical tables for electron detachment cross sections from H^- ions **75**

D.1 Collisions with helium atoms 76

D.2 Collisions with hydrogen atoms 77

D.3 Collisions with protons 78

D.4 Collisions with He^{+2} ions 79

D.5 Collisions with Li^{+3} ions 80

1 Introduction

The electron detachment (neutralization) processes from negative hydrogen ions (H^-) is important not only in basic collision physics but also in applied fields. For example, high energy ($\sim$ MeV), powerful ($\sim$ MW) neutral hydrogen atom (H^0) beam is often used in Neutral atom Beam Injection (NBI) for plasma heating. Also the neutral atom beam is used for diagnostics of plasma parameters such as ion density and temperature.

At such a high energy region, H^- ions can be converted into neutral hydrogen atoms more efficiently because the electron detachment cross sections from negative ions are generally larger than the electron capture cross sections into positive ions (protons). In order to get better understanding on such neutral hydrogen atom beam production processes it is necessary to study in detail the collision mechanisms of the electron detachment processes of H^- ions under various conditions.

A number of experimental investigations involving H^- ions had been reported so far and summarized by Tawara and Russek (1973). The calculated cross sections for electron detachment from H^- ion in fast atomic collisions have also been discussed in several reviews. For example, Gillespie (1977) calculated those based on the Born approximation. On the other hand, Bates and Walker (1967) used the classical impulse approximation and Dewangan and Walters (1978) used the free-collision model. Recently Riesselmann *et al.* (1991) used the free-collision classical impulse approximation. As the calculations of Gillespie (1977) and of Dewangan and Walters (1978) were based on so-called closure approximation in the matrix elements of the electron detachment part, then they considered only the sum of all product states of hydrogen atoms formed from H^- ions in the exit channel. Their results for total

cross sections are in reasonably good agreement with experimental data. Also very recently some partial cross sections for formation of the excited state hydrogen atoms (H^0) in the course of electron detachment from high energy (MeV) H^- ions have been measured by Radchenko and Ved'manov (1995). However, in these previous theoretical investigations, any contribution of the excited states of hydrogen atom in the exit channel was not discussed in detail.

In the first part of the present work, the first Born approximation is used to calculate the electron detachment cross section from H^- ions under neutral atom collisions. But, in contrast to these previous investigations, our calculations include more detailed matrix elements of transition probabilities of such electron detachment reactions. Firstly, we treat independently two electrons with different binding energies, namely 1s' and 1s electrons in H^- ion: one is the tightly bound electron (1s : ionization energy $\simeq$ 13.6 eV) and the other is the loosely bound electron (1s' : ionization energy $\simeq$ 0.75 eV) in the Hylleraas-Eckart function. So we take into account two different detachment processes, namely, i) detachment of the tightly bound (1s) electron and ii) detachment of the loosely bound (1s') electron. To describe more detail of the electron detachment processes, the binding energies of each electron are taken into account in the detached electron wave functions. Secondly, we consider the cross sections for production of hydrogen atoms not only in the ground state, $H^0(1s)$, but also in the excited states, $H^0(2s)$ and $H^0(2p)$, in the exit channel.

In the present calculations, the matrix elements of electron detachment processes for these two electrons are assumed to be independent of each other and depend on their initial binding energies in H^- ion. We then calculate the single-electron detachment cross sections for each of two electrons (1s and 1s') in H^- ions.

Then the present calculated results are compared and found to be in good agree-

ment with experimental data (Almeida *et al.* 1987, Anderson *et al.* 1980, Berkner *et al.* 1964, Dimov and Dudnikov 1967, Heinemeier *et al.* 1976, Kvale *et al.* 1995, Simpson and Gilbody 1972, Stier and Barnett 1956, Williams 1967) in high energy range.

In the second part of the present work, we also consider the single electron detachment processes from H^- ions colliding with positive ions. This process is important to obtain more powerful, high energy neutral beam with better conversion efficiencies. So far, very few experimental investigations of H^- ions colliding with positive ions have been reported only at low ($\leq$ 10keV/amu) energies mainly due to technical difficulties.

In this case, it is necessary to take into account the distortion effects for electrons in H^- ions due to the Coulomb field by positive ions. Previously Belkić (1997a, 1997b) calculated the single electron detachment cross sections from H^- ions in proton collisions based on the modified Coulomb-Born approximation. He used the Four-body Continuum Distorted Wave (4-B CDW) approximation to calculate the electron detachment cross sections, while using the plane wave to describe the detached electron in his calculation. We also use the 4-B CDW methods in the present calculations where we add the effects of the electric field of H^- ions. The present results clearly show that the electron detachment cross sections from H^- ions in collisions with positive ions (protons) are one order of magnitude larger than those with neutral hydrogen atoms and, thus, that H^- ions can be converted into neutral hydrogen atoms more efficiently through the electron detachment processes in collisions with positive ions than with neutral atoms.

We also discuss briefly the important consequences obtained in the present work

in applications to NBI.

In this thesis, in order to distinguish the converted neutral hydrogen atom from H^- ions from target hydrogen atom, we represent the former as H^0. Unless otherwise stated, we use the atomic units throughout the present paper.

References

Almeida D P, de Castro Faria N V, Freire, Jr F L, Montenegro E C and de Pinho A G, 1987 Phys. Rev. A **36**, 16

Anderson C J, Girnius R J, Howald A M and Anderson L W, 1980 Phys. Rev. A **22**, 822

Bates D R and Walker J C G, 1967 Proc. Phys. Soc. **90**, 333

Belkić Dž, 1997a Nucl. Instrum. Method. B **124**, 365

Belkić Dž, 1997b J. Phys. B **30**, 1731

Berkner K H, Kaplan S N and Pyle R V, 1964 Phys. Rev. **134**, 1461

Dimov G I and Dudnikov V G, 1967 Sov. Phys.-Tech. Phys. **11**, 919

Dewangan D P and Walters H R J, 1978 J. Phys. B **11**, 3983

Drukarev G F, 1970 Sov. Phys.-JETP **31**, 1193

Geddes J, Hill J and Gilbody H B, 1981 J. Phys. B **14**, 4837

Gillespie G H, 1977 Phys. Rev. **15**, 563

Heinemeier J, Hvelplund P and Simpson F R, 1976 J. Phys. B **9**, 2669

Kvale D P, Allen J S, Fang X D, Sen A and Matulioniene R, 1995 Phys. Rev. A **51**, 1351

Orbeli A L, Andreev E P, Ankudinov V A and Dukel'skii V M, 1970 Sov. Phys.-JETP **31**, 1044

Radchenko V I and Ved'manov G D, 1995 JETP **80**, 670

Riesselmann K, Anderson L W, Durand L and Anderson C J, 1991 Phys. Rev. A **43**, 5934

Simpson F R and Gilbody H B, 1972 J. Phys. B **5**, 1959

Shull H and Löwdin P-O, 1956 J. Chem. Phys. **25**, 1035

Stier P M and Barnett C F, 1956 Phys. Rev. **103**, 896

Tawara H and Russek A, 1973 Rev. Mod. Phys. **45**, 178

Williams J F, 1967 Phys. Rev. **154**, 9

2 Choice of wave functions

2.1 Wave function in the entrance channel

Firstly, we consider the electron wave function of negative hydrogen (H^-) ions in the unperturbed condition (in the asymptotic condition).

There are two electrons and one proton in H^- ion (see Figs. 3.1 and 4.1 later) and the interactions between two electrons are strong, Consequently two electrons in H^- ion have different binding energies: the first and second ionization energies are 0.75 eV and 13.6 eV, respectively. Thus, we define the coordinates of electrons in the entrance channel: $\boldsymbol{x}_1$ and $\boldsymbol{x}_2$ are the position vectors of two electrons relative to nucleus in H^- ion.

H^- ion is assumed to be in the ground state and can be described approximately by the Hylleraas-Eckart function (Shull and Löwdin 1955);

$$\Phi_{H^-}(\boldsymbol{x}_1, \boldsymbol{x}_2) = N_i(e^{-\alpha x_1}e^{-\beta x_2} + e^{-\beta x_1}e^{-\alpha x_2}) \tag{2.1}$$

$$\alpha = \nu(1-\mu), \quad \beta = \nu(1+\mu)$$

$$\nu = 0.6612, \quad \mu = 0.5717.$$

where N_i represents a normalization factor of the entrance channel, ν the scaling parameter and μ the split parameter. These parameters are given by Shull and Löwdin (1955). Equation (2.1) includes two different bound electrons in H^- ion, namely, one being the tightly bound state (1s) and the other the loosely bound state (1s'). α corresponds to the loosely bound electron and β the tightly bound electron. This structure indicates that the loosely bound electron moves around the hydrogenic system (the tightly bound electron plus proton).

2.2 Wave function in the exit channel

In the exit channel, namely after collisions, a H^- ion is transformed to a neutral hydrogen atom (H^0) and a detached electron. We have to take into account two effects here. Firstly, H^0 atoms are formed not only in the ground state, $H^0(1s)$, but also in the excited states, $H^0(2s)$ and $H^0(2p)$. Secondly, the detached electron moves under the influence of different effective charge of hydrogen-like system with different bound states in H^- ions (see Appendix A).

Now we define the coordinates of two electrons in the exit channel: $\boldsymbol{x}_1$ is an position vector of the electron still bound to H^0 relative to nucleus (proton) of H^0 and $\boldsymbol{x}_2$ the position vector of the detached electron relative to nucleus (proton) of H^0 (see Figs. 3.2 and 4.2 later).

Then, in such conditions, the wave functions can be represented with neutral hydrogen atom ($H^0(nlm)$) and the detached electron (e^-). We assume that electron coordinates $\boldsymbol{x}_1$ and $\boldsymbol{x}_2$ are independent of each other and, therefore, the form of the total wave function is given as the product of the detached electron wave function and the remaining electron in neutral hydrogen $H^0(nlm)$.

We use the hydrogenic function for the wave function of product neutral hydrogen atom, $H^0(nlm)$, n, l and m being the principal, azimuthal and magnetic quantum numbers, respectively (see Sec. 3.2 and Sec. 4.2).

On the other hand, the detached electron wave function is given as follows:

$$\phi_{e^-_{Z(j)}}(\boldsymbol{x}_i) = N(\zeta_{Z(j)})_1F_1\Big(i\zeta_{Z(j)}, 1, i(\kappa x_i - \boldsymbol{\kappa}\cdot\boldsymbol{x}_i)\Big)e^{i\boldsymbol{\kappa}\cdot\boldsymbol{x}_i} \tag{2.2}$$

$$N(\zeta_{Z(j)}) = \frac{\Gamma(1-\zeta_{Z(j)})e^{\pi\zeta_{Z(j)}}}{(2\pi)^{3/2}}$$

$$\zeta_{Z(j)} = \frac{Z(i)}{\kappa}, j = 1\mathrm{s} \text{ or } 1\mathrm{s}'. \tag{2.3}$$

where $Z(j)$ indicates the effective charge which each electron feels in H^- ion, namely $Z(1s)$ or $Z(1s')$ (see Appendix A). We consider two detached-electron wave functions, one corresponding to the tightly bound electron and the other the loosely bound electron. Here κ and $N(\zeta_{Z(j)})$ are the wave vector and a normalization factor of the detached electron wave function in the exit channel, respectively, ${}_1F_1$ the usual Kummer confluent hypergeometric function and Γ the gamma function.

Thus there are two different detachment processes of either 1s' or 1s electron (Imai *et al.* 1999), as indicated in the following :

$$\Phi_{H^-} \rightarrow \phi_{H^0(nlm)}\phi_{e^-_{Z(1s')}}, \quad \text{with} \quad Z(1s') = \sqrt{2I_{1s'}}, \tag{2.4}$$

$$\Phi_{H^-} \rightarrow \phi_{e^-_{Z(1s)}}\phi_{H^0(nlm)}, \quad \text{with} \quad Z(1s) = \sqrt{2I_{1s}} \quad . \tag{2.5}$$

Equation (2.4) represents the electron detachment process of the loosely bound electron and Eq. (2.5) the electron detachment process of the tightly bound electron in H^- ion. $I_{1s'}$ and I_{1s} indicate the ionization energies of the loosely and the tightly bound electrons in H^- ion. And the initial binding energies of each electron in the entrance channel are included in Eqs. (2.4) and (2.5).

References

Imai T W, Tawara H, Fainstein P and Rivarola R D, J. Phys. B **32**, 1247 (1999)

Shull H and Löwdin P -O, J. Chem. Phys. **25**, 1035 (1956)

3 Single electron detachment from H^- ions in collisions with neutral atoms (He and H)

3.1 Outline of present theory

Let us consider the electron detachment process of H^- ion moving with velocity $\boldsymbol{v}$ in collisions with neutral atoms (A), resulting in the production of neutral hydrogen atoms either in the ground state $H^0(1s)$ or in the excited states $H^0(2s)$ and $H^0(2p)$:

$$H^- + A(0) \quad \rightarrow \quad H^0(1s, 2s \text{ and } 2p) + e^- + \sum_{n'} A(n'). \tag{3.1}$$

On the L.H.S. of reaction (3.1), both particles (H^- and A(0)) are assumed to be in the ground state in the entrance channel. The third term on the R.H.S. of reaction (3.1) indicates the summation over all the possible states (n') of target atoms including the ionization in the exit channel.

We calculate the cross sections for reaction (3.1) based on the Plane-Wave-Born-Approximation (PWBA) over H^- ion incident energy ranging from 10 keV to 10 MeV, which is important in NBI and plasma diagnostics.

We do not need to take into account any distortion effect in reaction (3.1) as it is not important in interactions with neutral target atoms, A(0).

A lot of PWBA calculations for various atomic collisions had been performed so far. PWBA is basically the perturbation theory and, in this way, is a good treatment for high velocity collisions ($\sim$ 25keV/amu). As mentioned in Sec.2.1, we introduced the parameters of the binding energies of two electrons (1s and 1s') in H^- ions for the detached electron wave function in PWBA and, thus, there are two different electron detachment processes.

3.2 Calculations

The total Hamiltonian of reaction (3.1) is given by

$$H = -\frac{\nabla^2_{\boldsymbol{R}}}{2M} - \frac{\nabla^2_{\boldsymbol{x}_1}}{2} - \frac{\nabla^2_{\boldsymbol{x}_2}}{2} - \frac{1}{x_1} - \frac{1}{x_2} + \frac{1}{x_{12}} + \sum_j \sum_{j \neq j'} \Big[-\frac{\nabla^2_{\boldsymbol{s}_j}}{2} - \frac{Z_T}{s_j} + \frac{1}{s_{jj'}} \Big] + V, \tag{3.2}$$

where M is the reduced mass of H^- ion system, x_{12} and $s_{jj'}$ are the electron-electron distances in H^- ion and in neutral atom, respectively. We denote the detailed description of this coordinate system in Fig. 3.1 and Fig. 3.2. The first term in Eq. (3.2) represents the kinetic energy of H^- ion, the second to sixth terms the kinetic and the potential energies of two electrons in H^- ion and the seventh to ninth terms the kinetic and the potential energies of electrons in neutral target atoms (nuclear charge, Z_T). The last term is the perturbation between H^- ion and the neutral target atom and is given by

$$V = \frac{Z_T}{R} - \Big[\frac{Z_T}{|\boldsymbol{R} - \boldsymbol{x}_1|} + \frac{Z_T}{|\boldsymbol{R} - \boldsymbol{x}_2|} \Big] + \sum_j \Big[-\frac{1}{|\boldsymbol{R} + \boldsymbol{s}_j|} + \frac{1}{|\boldsymbol{R} + \boldsymbol{s}_j - \boldsymbol{x}_1|} + \frac{1}{|\boldsymbol{R} + \boldsymbol{s}_j - \boldsymbol{x}_2|} \Big], \tag{3.3}$$

where the first term in Eq. (3.3) corresponds to the interaction between nucleus (proton) in H^- ion and nucleus of neutral target atom, the second and third terms the interaction between nucleus of neutral target atom and two electrons in H^- ion, the fourth term the interaction between proton in H^- ion and electrons in neutral target atom, and the last two terms the interaction between two electrons in H^- ion and electrons in neutral target atom (see Fig. 3.1).

The wave function of total system in the entrance channel is given as follows:

$$\Psi_i = \Phi_{H^-}(\boldsymbol{x}_1, \boldsymbol{x}_2) T_0(\boldsymbol{s}_j) e^{i\boldsymbol{k}_i \cdot \boldsymbol{R}} \tag{3.4}$$

where $\boldsymbol{k}_i$ (parallel to $\boldsymbol{v}$) is the initial momentum of H^- ion, $\boldsymbol{R}$ the inter-nuclei coordinate and T_0 represents the target state (ground state) in the entrance channel and Φ_{H^-} the wave function of H^- ion (see Sec.3.1).

On the other hand, the total wave function in the exit channel, Ψ_f, is given as follows:

$$\Psi_f(\boldsymbol{x}_1, \boldsymbol{x}_2) = \Phi_{H^0(nlm), e^-_{Z(i)}}(\boldsymbol{x}_1, \boldsymbol{x}_2) T_{n'}(\boldsymbol{s}_j) e^{i\boldsymbol{k}_f \cdot \boldsymbol{R}}, \tag{3.5}$$

$$Z(i) = 1s \text{ or } 1s'$$

where $\boldsymbol{k}_f$ is the final momentum of neutral hydrogen atom (H^0). $\Phi_{H^0(nlm), e^-_{Z(i)}}$ is the wave function for a system consisting of $H^0(nlm)$ atom and the detached electron $e^-_{Z(i)}$ system (see Sec.2.2). Here we treat the electron detachment processes of both electrons coordinates $\boldsymbol{x}_1$ and $\boldsymbol{x}_2$ and, then, the wave function in the exit channel is given as follows:

$$\Phi_{H^0(nlm), e^-_{Z(i)}} = \frac{N_f}{\sqrt{2}} [\phi_{e^-_{Z(i)}}(\boldsymbol{x}_1) \phi_{H^0(nlm)}(\boldsymbol{x}_2) + \phi_{e^-_{Z(i)}}(\boldsymbol{x}_2) \phi_{H^0(nlm)}(\boldsymbol{x}_1)]. \tag{3.6}$$

And $T_{n'}(\boldsymbol{s}_j)$ in Eq. (3.5) represents the target states in the exit channel.

As the present calculations are based on the PWBA, the cross section can be written by

$$\begin{aligned} \sigma &= \sum_{nlm} \sum_{n'} \frac{M^2}{4\pi} \int \int_0^{\kappa_{max}} |f|^2 d\Omega d\boldsymbol{\kappa} \\ &= \sum_{nlm} \sum_{n'} \frac{1}{4\pi v^2} \int_{q_{min}}^{q_{max}} \int_0^{\kappa_{max}} |f(\boldsymbol{q})|^2 dq d\boldsymbol{\kappa}, \end{aligned} \tag{3.7}$$

where the summation in Eq. (3.7) is performed over all neutral hydrogen atom states ($H^0(nlm)$) and also over all states ($T(n')$) of the neutral target atom in the exit channel, v the incident velocity of H^- ion, q_{min} and q_{max} the minimum and

maximum momentum transfers, κ_{max} the maximum momentum of the detached electron and $\boldsymbol{q}$ denotes the momentum transfer

$$\boldsymbol{q} = \boldsymbol{k}_i - \boldsymbol{k}_f, \tag{3.8}$$

with the wave number of the detached electron with $\boldsymbol{\kappa}$. In Eq. (3.7), $f(\boldsymbol{q})$ is the matrix element given as follows:

$$\begin{aligned} f(\boldsymbol{q}) &= -\int \langle \Psi_f | V | \Psi_i \rangle d\boldsymbol{R} \\ &= -\int \langle \Phi_{H^0(nlm),e^-_{Z(i)}}(\boldsymbol{x}_1,\boldsymbol{x}_2) T_{n'}(\boldsymbol{s}_j) | V | \Phi_{H^-}(\boldsymbol{x}_1,\boldsymbol{x}_2) T_0(\boldsymbol{s}_j) \rangle e^{i\boldsymbol{q}\cdot\boldsymbol{R}} d\boldsymbol{R}. \end{aligned} \tag{3.9}$$

Using the Bethe integral (Bethe and Jackiw 1968), Eq. (3.3) can be written as follows:

$$V = \int \frac{d\boldsymbol{q}}{q^2}\Big[Z_T\{1 - e^{-i\boldsymbol{q}\cdot\boldsymbol{x}_1} - e^{-i\boldsymbol{q}\cdot\boldsymbol{x}_2}\} - \sum_j \{e^{i\boldsymbol{q}\cdot\boldsymbol{s}_j} + e^{i\boldsymbol{q}\cdot(\boldsymbol{s}_j-\boldsymbol{x}_1)} + e^{i\boldsymbol{q}\cdot(\boldsymbol{s}_j-\boldsymbol{x}_2)}\}\Big]. \tag{3.10}$$

Substituting Eq. (3.10) into Eq. (3.9),

$$\begin{aligned} f(\boldsymbol{q}) &= \int \frac{d\boldsymbol{q}}{q^2} \langle \Phi_{H^0(nlm),e^-_{Z(j)}}(\boldsymbol{x}_1,\boldsymbol{x}_2) T_{n'}(\boldsymbol{s}_j) | (1 - e^{-i\boldsymbol{q}\,\boldsymbol{x}_1} - e^{-i\boldsymbol{q}\,\boldsymbol{x}_2}) \\ &\quad \times (Z_T - \sum_j e^{i\boldsymbol{q}\cdot\boldsymbol{s}_j}) | \Phi_{H^-} T_0(\boldsymbol{s}_j) \rangle. \end{aligned} \tag{3.11}$$

Equation (3.11) can be separated into two factors corresponding to H^- ion and neutral atom systems:

$$F_p(\boldsymbol{q},\boldsymbol{\kappa}) = \langle \Phi_{H^0(nlm),e^-_{Z(j)}}(\boldsymbol{x}_1,\boldsymbol{x}_2) | 1 - e^{-i\boldsymbol{q}\cdot\boldsymbol{x}_1} - e^{-i\boldsymbol{q}\cdot\boldsymbol{x}_2} | \Phi_{H^-}(\boldsymbol{x}_1,\boldsymbol{x}_2) \rangle \tag{3.12}$$

$$F_{n'0}(\boldsymbol{q}) = \langle T_{n'}(\boldsymbol{s}_j) | Z_T - \sum_j e^{i\boldsymbol{q}\cdot\boldsymbol{s}_j} | T_0(\boldsymbol{s}_j) \rangle. \tag{3.13}$$

Equations (3.12) and (3.13) represent the form factors of H^- ion system and of neutral target atom system, respectively.

Then the total cross section is given by

$$\sigma = \frac{1}{8\pi v^2} \sum_{nlm} \sum_{n'} \int_{q_{min}}^{q_{max}} \int_0^{\kappa_{max}} |F_p(\boldsymbol{q}, \boldsymbol{\kappa})|^2 |F_{n'0}(\boldsymbol{q})|^2 \frac{dq}{q^3} d\boldsymbol{\kappa}. \tag{3.14}$$

Furthermore, the H^- ion factor, Eq. (3.12), can be separated into two matrix elements, one being the electron detachment part and the other the remaining neutral hydrogen atom. As mentioned in Sec.2.2, there are two processes for single electron detachment and, then, we assume that single electron detachment processes for two electrons in H^- ion are independent of each other and, therefore,

$$\begin{aligned} |F_p(\boldsymbol{q}, \boldsymbol{\kappa})|^2 = \quad & |F_p(\boldsymbol{q}, \boldsymbol{\kappa})(1\mathrm{s} \rightarrow \mathrm{e}^-, 1\mathrm{s}' \rightarrow \mathrm{H}^0(nlm))|^2 \\ + \quad & |F_p(\boldsymbol{q}, \boldsymbol{\kappa})(1\mathrm{s}' \rightarrow \mathrm{e}^-, 1\mathrm{s} \rightarrow \mathrm{H}^0(nlm))|^2 \end{aligned} \tag{3.15}$$

where the first term on R.H.S. denotes that the 1s electron is detached, meanwhile the $1s'$ electron remains in neutral hydrogen atom forming $H^0(nlm)$ and the second term on R.H.S. that the 1s' electron is detached and the 1s electron remains in neutral hydrogen atom. We assume also that two electron coordinates, $\boldsymbol{x}_1$ and $\boldsymbol{x}_2$, are independent of each other. Then the first and second terms in Eq. (3.15) can be separated into two parts, namely the electron detachment part, which had already been introduced by Belkić (1984) in one electron systems, and the form factors of H^- ion system as follows (Gradshteyn and Ryzhik 1994):

$$\begin{aligned} & F_p(\boldsymbol{q}, \boldsymbol{\kappa})(1\mathrm{s}' \rightarrow \mathrm{e}^-, 1\mathrm{s} \rightarrow \mathrm{H}^0(nlm)) \\ = \; - \; & N_i N_f^* \Big[\frac{4\pi\alpha}{\kappa^2 + \alpha^2} \Big(1 + \frac{2\boldsymbol{\kappa} \cdot \boldsymbol{\kappa} - i2\kappa\alpha}{\kappa^2 + \alpha^2} \Big)^{-i\zeta_{Z(1s')}} F_{p2}(\beta) \\ & - \frac{4\pi\alpha}{\kappa^2 + \alpha^2} \Big(1 + \frac{2\boldsymbol{\kappa} \cdot \boldsymbol{\kappa} - i2\kappa\alpha}{\kappa^2 + \alpha^2} \Big)^{-i\zeta_{Z(1s')}} F_{p2}(\boldsymbol{q}, \beta) \\ & - \frac{4\pi\alpha}{p^2 + \alpha^2} \Big(1 + \frac{2\boldsymbol{p} \cdot \boldsymbol{\kappa} - i2\kappa\alpha}{p^2 + \alpha^2} \Big)^{-i\zeta_{Z(1s')}} F_{p2}(\beta) \Big] \end{aligned} \tag{3.16}$$

and

$$
\begin{aligned}
& F_p(\boldsymbol{q},\boldsymbol{\kappa})(1s \rightarrow e^-, 1s' \rightarrow H^0(nlm)) \\
- \; - \; & N_i N_f^* \Big[\frac{4\pi\beta}{\kappa^2+\beta^2}\Big(1+\frac{2\boldsymbol{\kappa}\cdot\boldsymbol{\kappa}-i2\kappa\beta}{\kappa^2+\beta^2}\Big)^{-i\zeta_{Z(1s)}} F_{p2}(\alpha) \\
& -\frac{4\pi\beta}{\kappa^2+\beta^2}\Big(1+\frac{2\boldsymbol{\kappa}\cdot\boldsymbol{\kappa}-i2\kappa\beta}{\kappa^2+\beta^2}\Big)^{-i\zeta_{Z(1s)}} F_{p2}(\boldsymbol{q},\alpha) \\
& -\frac{4\pi\beta}{p^2+\beta^2}\Big(1+\frac{2\boldsymbol{p}\cdot\boldsymbol{\kappa}-i2\kappa\beta}{p^2+\beta^2}\Big)^{-i\zeta_{Z(1s)}} F_{p2}(\alpha)\Big]
\end{aligned}
\tag{3.17}
$$

where $\boldsymbol{p}$ denotes the sum of momentum transfer, $\boldsymbol{q}$, and the wave number of the detached electron, $\boldsymbol{\kappa}$:

$$
\boldsymbol{p} = \boldsymbol{q} + \boldsymbol{\kappa}. \tag{3.18}
$$

In Eqs. (3.16) and (3.17), $F_{p2}(\alpha)$, $F_{p2}(\boldsymbol{q},\alpha)$, $F_{p2}(\beta)$ and $F_{p2}(\boldsymbol{q},\beta)$ denote the matrix element parts of an electron-remaining in $H^0(nlm)$:

$$
F_{p2}(\lambda) = \int d\boldsymbol{x}\phi_{H^0(nlm)}(\boldsymbol{x})e^{-\lambda x} \tag{3.19}
$$

$$
F_{p2}(\boldsymbol{q},\lambda) = \int d\boldsymbol{x}\phi_{H^0(nlm)}(\boldsymbol{x})e^{i\boldsymbol{q}\cdot\boldsymbol{x}}e^{-\lambda x} \tag{3.20}
$$

where

$$
\lambda = \alpha \text{ or } \beta. \tag{3.21}
$$

(see Eq. 2.1).

On the other hand, the neutral target atom form factor, Eq. (3.13), can also be separated into two terms, one being the neutral atom left in the ground state, T(0), and the other the neutral atom excited state, T(n'), in the exit channel and, assuming that they are independent, total cross sections are given as the sum of these two terms,

$$
\sigma = \sigma_{00} + \sigma_{n'0}, \tag{3.22}
$$

where

$$\sigma_{00} = \sum_{nlm} \overline{8\pi v^2} \int_{q_{min}}^{q_{max}} \int_0^{\kappa_{max}} |F_p(\boldsymbol{q},\boldsymbol{\kappa})|^2 |F_{00}|^2 \frac{dq}{q^3} d\boldsymbol{\kappa} \quad (3.23)$$

$$\sigma_{n'0} = \sum_{nlm} \overline{8\pi v^2} \int_{q_{min}(\Delta\varepsilon)}^{q_{max}} \int_0^{\kappa_{max}(\Delta\varepsilon)} |F_p(\boldsymbol{q},\boldsymbol{\kappa})|^2 \sum_{n'\neq 0} |F_{n'0}|^2 \frac{dq}{q^3} d\boldsymbol{\kappa} \quad (3.24)$$

$$|F_{00}|^2 = |\langle T_0(\boldsymbol{s}_j)| Z_T - \sum_j e^{i\boldsymbol{q}\cdot\boldsymbol{s}_j} |T_0(\boldsymbol{s}_j)\rangle|^2 \quad (3.25)$$

$$\sum_{n'\neq 0} |F_{n'0}|^2 = \sum_{n'\neq 0} |\langle T_{n'}(\boldsymbol{s}_j)| \sum_j e^{i\boldsymbol{q}\cdot\boldsymbol{s}_j} |T_0(\boldsymbol{s}_j)\rangle|^2. \quad (3.26)$$

Equations (3.24) and (3.26) should be summed over all product states (n') of neutral atom target in the exit channel. But it is time-consuming to calculate those for all product states of neutral target atoms. Therefore, the closure approximation is used for summing over the final state (Dmitriev and Nikolaev 1963, Victor 1969, Levy 1969, Lodge 1969, Belkić and Gayet 1975, Rule 1977, Gillespie 1977, Dewangan and Walters 1978, Briggs and Drepper 1978, Briggs and Day 1980, Kaminsky *et al.* 1980, McGuire *et al.* 1981, Day 1981, Anholt 1986, Hartley and Walters 1987, Montenegro and Meyerhof 1991, Montenegro *et al.* 1994). Thus, we can rewrite Eq. (3.26) into the following form :

$$\sum_{n'} |\, F_{n'0}(\boldsymbol{q})\,|^2 = |\,\langle T_0(\boldsymbol{s}_j)| \sum_j \sum_{j'} e^{i\boldsymbol{q}\cdot\boldsymbol{s}_j} e^{-i\boldsymbol{q}\cdot\boldsymbol{s}_{j'}} |T_0(\boldsymbol{s}_j)\rangle\,| - |\,\langle T_0(\boldsymbol{s}_j)| \sum_j e^{i\boldsymbol{q}\cdot\boldsymbol{s}_1} |T_0(\boldsymbol{s}_j)\rangle\,|^2 . \quad (3.27)$$

The closure approximation has some merits: i) it is not necessary to individually calculate all states of neutral atom, ii) it is easy to lead the matrix elements of $F_{n'0}$ and iii) the closure relation includes all the states of neutral atom target.

However, introducing the closure approximation accompanies another problem. In Eqs. (3.23) and (3.24), the minimum momentum transfers, q_{min} and $q_{min}(\Delta\varepsilon)$,

are given as

$$q_{min} = \frac{I_p}{v} \tag{3.28}$$

$$q_{min}(\Delta\varepsilon) = \frac{I_p + \Delta\varepsilon}{v} \tag{3.29}$$

where I_p is the energy transfer from H^- ion to $H^0(nlm)$ atom :

$$I_p = E_{H^0(nlm)} - E_{H^-}, \tag{3.30}$$

with $E_{H^0(nlm)}$ being the eigenenergy of $H^0(nlm)$ atom in the exit channel, E_{H^-} the eigenenergy of H^- ion in the entrance channel and $\Delta\varepsilon$ the average excitation energy of the neutral target atom. The maximum and minimum of κ-integral in Eqs. (3.23) and (3.24), κ_{max}, $\kappa_{max}(\Delta\varepsilon)$ and κ_{min}, are given as follows :

$$\kappa_{max} = \sqrt{2v}\sqrt{q - q_{min}} \tag{3.31}$$

$$\kappa_{max}(\Delta\varepsilon) = \sqrt{2v}\sqrt{q - q_{min}(\Delta\varepsilon)} \tag{3.32}$$

$$\kappa_{min} = 0. \tag{3.33}$$

In the closure approximation, the average excitation energy is not clearly defined because the closure relation includes all states (except for the ground state) of neutral target atoms.

For this problem, Montenegro and Meyerhof (1991) and Montenegro *et al.* (1994) proposed the average value of excitation energy of target based on the Bethe sum rule for energy loss (Bethe and Jackiw 1968),

$$q_{min}(\Delta\varepsilon) = q_{min} + \frac{q_{min}^2(1 + q_{min}/2v)^2 Z_T}{2v}. \tag{3.34}$$

Finally, we summed the calculated cross sections of the production of $H^0(2p)$ over all the magnetic quantum numbers of 2p states, namely,

$$\sigma(2p) = \sigma(21-1) + \sigma(210) + \sigma(211), \tag{3.35}$$

In Sec.3.3, we will present the calculated results and detailed discussion on comparison with experimental data available.

3.3 Results and discussion

Using Eq. (3.22), we have computed the electron detachment cross sections for H^- ions in collisions with neutral helium and hydrogen atoms in detail. In this section, we discuss and compare our calculated results of partial as well as total cross sections with experimental data for process (3.1) mentioned above.

It should be noted that so far no theories had shown any partial cross sections for H^0 atom formed in the electron detachment processes from H^- ions.

3.3.1 Colliding with helium atoms

In this section, we show the calculated results in colliding with neutral helium atoms;

$$H^- + He(0) \quad \rightarrow \quad H^0(1s, 2s \text{ and } 2p) + e^- + \sum_{n'} He(n'). \tag{3.36}$$

In order to describe neutral helium target, we use the Roothan-Hartree-Fock Functions (Clementi and Roetti 1974) in the present calculations.

Numerical cross section data calculated are given in Appendix D.1.

Figure 3.3 displays some partial cross sections corresponding to the formation of $H^0(1s)$, $H^0(2s)$ and $H^0(2p)$ atoms as well as total cross sections of the electron detachment process from H^- ion colliding with He atoms. As can be seen in Fig. 3.3, when one of the electrons in H^- ion is detached, the calculated cross sections for the formation of the ground state hydrogen atom, $H^0(1s)$, are dominant in all the collision energy range investigated. In Fig. 3.3 some important consequences are noticed. Firstly, the cross sections for formation of $H^0(2s)$ atom is roughly 50 % larger than those for $H^0(2p)$ atom in high energy (> 100 keV) region and, secondly, $H^0(2s)$ atom formation is found to account for about 20 % and $H^0(2p)$ atom formation about 10 % of total electron detachment cross sections.

We also compare our calculated partial cross sections with experimental data which are taken from Geddes *et al.* (1981), Orbeli *et al.* (1970) and Radchenko and Ved'manov (1995). In particular, our results are in good agreement with experimental data by Radchenko and Ved'manov at MeV energy range. However, in low energy (< 30 keV) region, the observed electron detachment cross sections for production of $H^0(2s)$ become smaller than those for production of $H^0(2p)$, which is in sharp contrast with our calculated results. This difference can be understood, as discussed by Risley *et al.* (1978), due to the fact that the electron detachment at low energies proceeds via so-called electron promotion mechanism through formation of a quasi-molecule where the excitation to the 2p state is favorable over that to the 2s state. In the present calculation this mechanism has not been included.

The present calculations clearly show that the formation of the excited state hydrogen atoms, $H^0(2s)$ and $H^0(2p)$, is an important and non-negligible process in high energy region, suggesting that neutralization efficiencies of H^- ions in applications to NBI (see Introduction) will be significantly influenced by these neutral hydrogen

atoms in the excited states, which are easily ionized than those in the ground state.

In order to understand the contribution of two electrons with different binding energies in H^- ion to electron detachment processes, Fig. 3.4 displays partial cross sections of electron detachment processes:

$$1s' \rightarrow e^-, 1s \rightarrow H^0(1s) \tag{3.37}$$

$$1s \rightarrow e^-, 1s' \rightarrow H^0(1s) \tag{3.38}$$

where Eq. (3.37) indicates the processes where the loosely bound (1s') electron is detached, meanwhile the tightly bound electron (1s) remains in the 1s orbit of the neutral hydrogen atom, and, on the other hand, Eq. (3.38) those where the tightly bound electron (1s) is detached, meanwhile the loosely bound electron (1s') remains in the 1s orbit of the neutral hydrogen atom. In production of the ground state hydrogen atom, $H^0(1s)$, the detachment process from the loosely bound electron (1s) (solid-curve) is dominant over that from the tightly bound electron (1s') (dotted-curve), as expected.

We show similar results of the production for $H^0(2s)$ and $H^0(2p)$ atoms. Figure 3.5 displays partial cross sections of electron detachment processes:

$$1s' \rightarrow e^-, 1s \rightarrow H^0(2s) \tag{3.39}$$

$$1s \rightarrow e^-, 1s' \rightarrow H^0(2s) \tag{3.40}$$

where Eq. (3.39) indicates those where the loosely bound electron (1s') is detached, meanwhile the tightly bound electron (1s) is excited to the 2s orbit of neutral hydrogen atom (solid-curve) and Eq. (3.40) those where the tightly bound electron (1s)

is detached, meanwhile the loosely bound electron (1s') is excited to the 2s orbit of the neutral hydrogen atom (dotted-curve).

Figure 3.6 displays partial cross sections of electron detachment processes:

$$1s' \rightarrow e^-, 1s \rightarrow H^0(2p) \tag{3.41}$$

$$1s \rightarrow e^-, 1s' \rightarrow H^0(2p) \tag{3.42}$$

where Eq. (3.41) indicates those where the loosely bound electron (1s') is detached, meanwhile the tightly bound electron (1s) is excited to the 2p orbit of the neutral hydrogen atom (solid-curve) and Eq. (3.42) those where the tightly bound electron (1s) is detached, meanwhile the loosely bound electron (1s') is excited to the 2p orbit of the neutral hydrogen atom (dotted-curve).

In Figs. 3.5 and 3.6, it is interesting to note that, in formation of the excited state hydrogen atoms, $H^0(2s)$ and $H^0(2p)$, Drukarev (1970) and Orbeli *et al.* (1970) suggested quite some time ago that the process, where the 1s electron is detached while the 1s' electron is excited, can be dominant over that, where the 1s' electron is detached while the 1s electron is excited. When the nuclear screening is suddenly changed after the 1s electron detachment, the loosely bound 1s' electron favorably goes to the 2s or 2p states, producing $H^0(2s)$ and $H^0(2p)$ atoms because their energy levels are close to the 1s' electron energy level in H^- ion. In high energy region, our results are consistent with this mechanism. But in low energy region as seen in Fig. 3.6, the present calculated results for the production of $H^0(2p)$ atoms are not consistent with their explanation. This disagreement may come from the Hylleraas-Eckart function (Eq. (2.1)) which we used because this function does not include the orbital angular momentum part, meanwhile the hydrogenic wave function of 2p state includes this part and, then, Eq. (3.19) is canceled out in the cross section

for the production of $H^0(2p)$ atoms. The final forms of Eq. (3.20) are different in the production $H^0(2s)$ and $H^0(2p)$ atoms. The influence of different forms between $H^0(2s)$ and $H^0(2p)$ is very large near the lower limit q_{min}.

Figure 3.7 displays a comparison of the present calculated results for total electron detachment cross sections with the results previously calculated by Dewangan and Walters (1981), Riesselmann *et al.* (1991) and also with experimental data. The experimental data points are taken from Almeida *et al.* (1987), Anderson *et al.* (1980), Berkner *et al.* (1964), Dimov and Dudnikov (1967), Heinemeier *et al.* (1976), Kvale *et al.* (1995), Simpson and Gilbody (1972), Stier and Barnett (1956) and Williams (1967). Our calculated results of the total cross sections summed over three processes including formation of the ground state hydrogen atom, $H^0(1s)$, and the excited states hydrogen atoms, $H^0(2s)$ and $H^0(2p)$, are in a good agreement with the experimental data available, except for those at the lowest energies where the Born approximation is known to break down and also with the previously calculated results based on different calculations over the present collision energy range.

3.3.2 Colliding with hydrogen atoms

In this section, we show similar results for electron detachment from H^- ions colliding with neutral (ground state) hydrogen atom target, H(0),

$$H^- + H(0) \quad \rightarrow \quad H^0(1s, 2s \text{ and } 2p) + e^- + \sum_{n'} H(n'). \tag{3.43}$$

We use the hydrogen wave function for target hydrogen atoms.

Numerical cross section data calculated are given in Appendix D.2.

Figure 3.8 shows partial cross sections corresponding to the formation of $H^0(1s)$, $H^0(2s)$ and $H^0(2p)$ atoms as well as total cross sections of electron detachment process from H^- ion colliding with hydrogen atom. Comparing Fig. 3.8 with Fig. 3.3, we note the results similar to those in helium atom. Namely, at high energies ($>$ 100keV), cross sections for $H^0(2s)$ formation is found to account for about 20 % and those for $H^0(2p)$ formation about 10 % of total electron detachment cross sections. Unfortunately, there is no experimental data of partial cross sections to be compared with the present calculated results.

The present results for atomic hydrogen targets also show that the inclusion of the excited state neutral hydrogen, $H^0(2s)$ and $H^0(2p)$, converted from H^- ions in the exit channel is important in many applications.

Figure 3.9 displays partial cross sections of electron detachment with neutral hydrogen atom processes:

$$1s' \rightarrow e^-, 1s \rightarrow H^0(1s) \tag{3.44}$$

$$1s \rightarrow e^-, 1s' \rightarrow H^0(1s). \tag{3.45}$$

The notations are already given in the previous section (see Eqs. (3.37) and 3.38)). In production of the ground state hydrogen atom, $H^0(1s)$, the detachment process of the loosely bound electron (1s) (solid-curve) is also dominant over that from the tightly bound state(1s') (dotted-curve) in conversion from H^- ions.

We also show the results for production of $H^0(2s)$ and $H^0(2p)$ atoms. Figure 3.10 displays partial cross sections of electron detachment processes:

$$1s' \rightarrow e^-, 1s \rightarrow H^0(2s) \tag{3.46}$$

$$1s \rightarrow e^-, 1s' \rightarrow H^0(2s). \tag{3.47}$$

In Fig. 3.10, the solid-curve indicates those for process (3.46) and the dotted-curve those for process (3.47).

Similarly, Fig. 3.11 displays partial cross sections of electron detachment processes:

$$1s' \rightarrow e^-, 1s \rightarrow H^0(2p) \tag{3.48}$$

$$1s \rightarrow e^-, 1s' \rightarrow H^0(2p). \tag{3.49}$$

In Fig. 3.11, the solid-curve indicates those for process (3.48) and dotted-curve those for process (3.49).

Qualitative explanation on the dominance of 2s and 2p state formation from the loosely bound electron (1s'), while 1s electron is detached, has been given by Drukarev (1970) and Orbeli *et al.* (1970), as discussed in the previous section. The present results for cross sections of formation of the excited state hydrogen atoms, $H^0(2s)$ and $H^0(2p)$, in collisions with atomic hydrogen target are practically the same as those in neutral helium atom target.

Finally, we show the total cross sections in Fig. 3.12. The experimental data points are taken from Hvelplund and Andersen (1987) and Geddes *et al.* (1980). Our calculated results of the total cross sections summed over three processes including formation of the ground state hydrogen atom, $H^0(1s)$, and the excited state hydrogen atoms, $H^0(2s)$ and $H^0(2p)$, are in good agreement with the experimental data, confirming that the present calculation method can provide reasonably accurate cross sections for single electron detachment from H^- ions in collisions with neutral atoms at high energies.

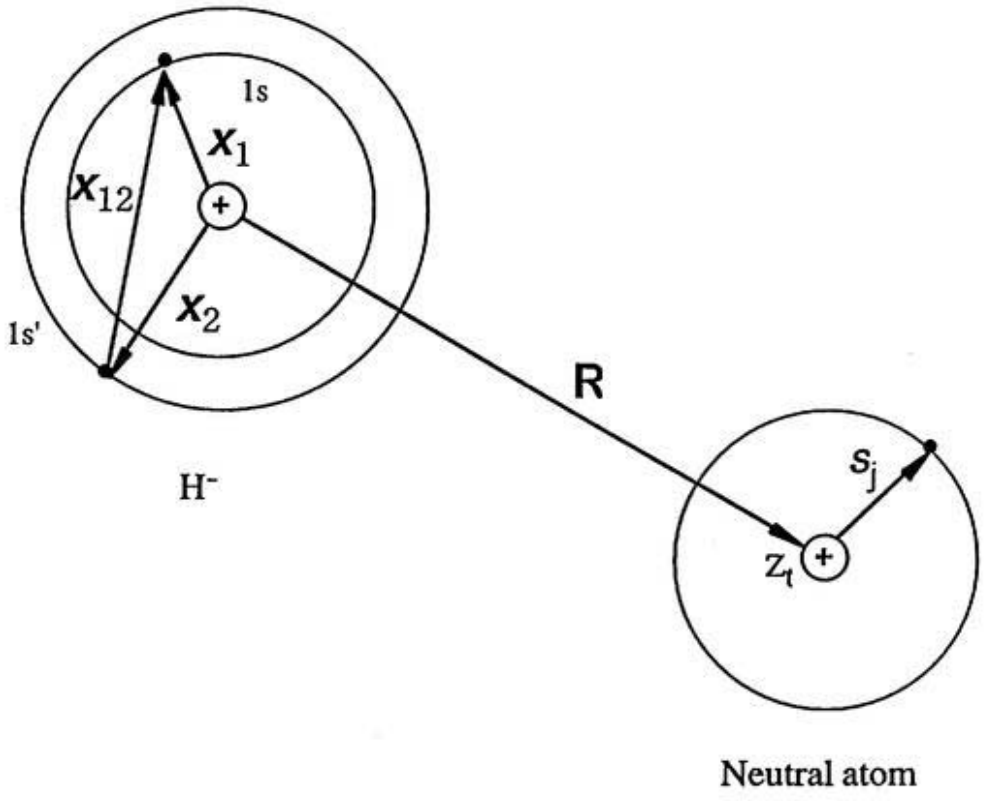

Figure 3.1: The coordinate system of the entrance channel

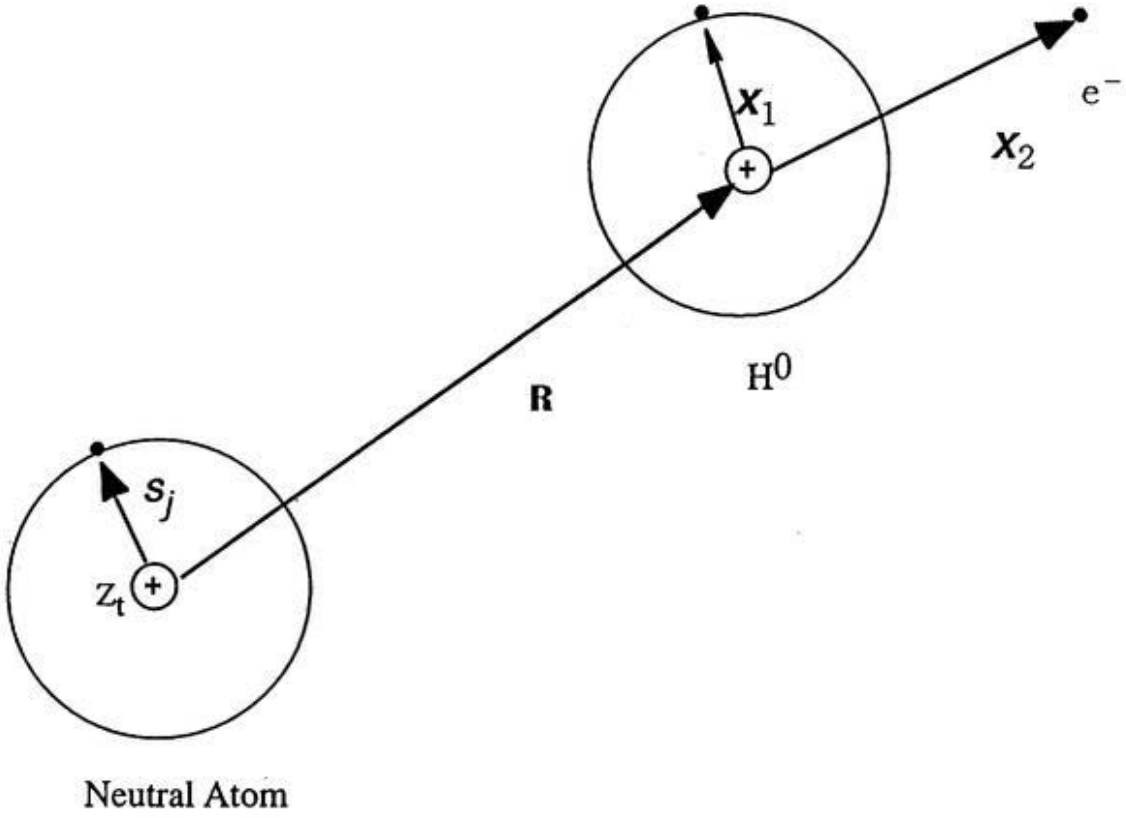

Figure 3.2: The coordinate system of the exit channel

$$H^- + He(0) \quad \rightarrow \quad H^0(1s, 2s \text{ and } 2p) + e^- + \sum_{n'} He(n')$$

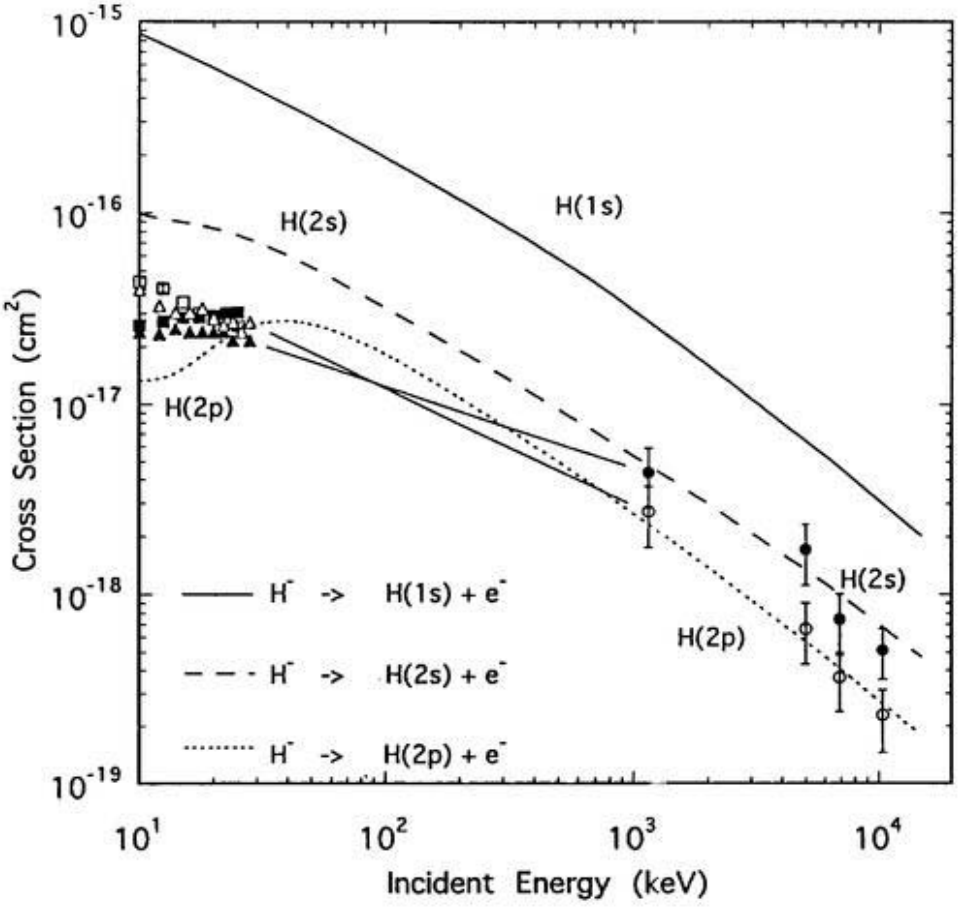

Figure 3.3: Partial cross sections of single electron detachment processes from H^- ions in collisions with neutral helium atom target, forming hydrogen atoms in the ground state, $H^0(1s)$, and the excited states, $H^0(2s)$ and $H^0(2p)$. The symbols represent experimental data of Geddes *et al.* (solid square), Orbeli *et al.* (solid triangle) and Radchenko *et al.* (solid circle) for production of $H^0(2s)$ in the exit channel and Geddes *et al.* (open square), Orbeli *et al.* (open triangle) and Radchenko *et al.* (open circle) for production of $H^0(2p)$ in the exit channel. The solid-curve represents the calculated cross sections for production of hydrogen atom in the ground state, $H^0(1s)$, the dashed-curve those for the excited 2s state, $H^0(2s)$, and the dotted-curve those for the excited 2p state, $H^0(2p)$.

$$H^- + He(0) \quad \rightarrow \quad H^0(1s) + e^- + \sum_{n'} He(n')$$

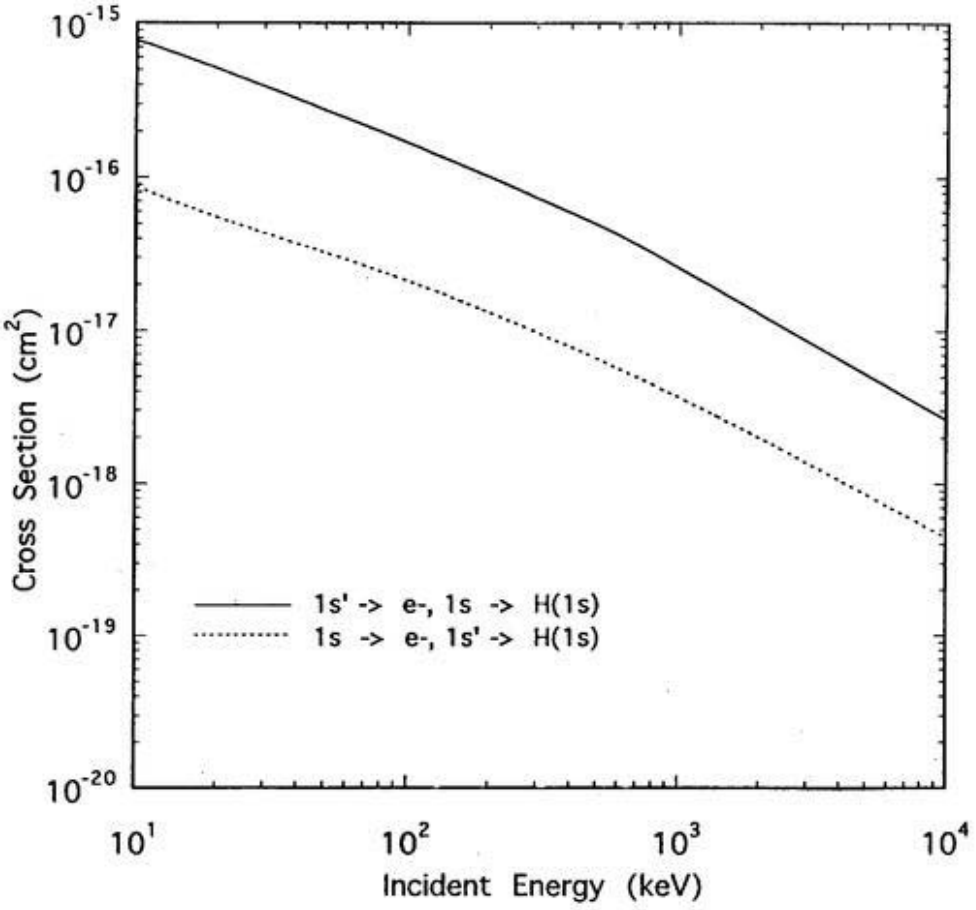

Figure 3.4: Calculated partial cross sections for formation of the ground state hydrogen atoms. The solid-curve represents those for hydrogen atom in the ground state $H^0(1s)$ accompanied with the loosely bound 1s' electron detached and the dotted-curve those for hydrogen atom in the ground state $H^0(1s)$ accompanied with the tightly bound 1s electron detached.

$$H^- + He(0) \quad \rightarrow \quad H^0(2s) + e^- + \sum_{n'} He(n')$$

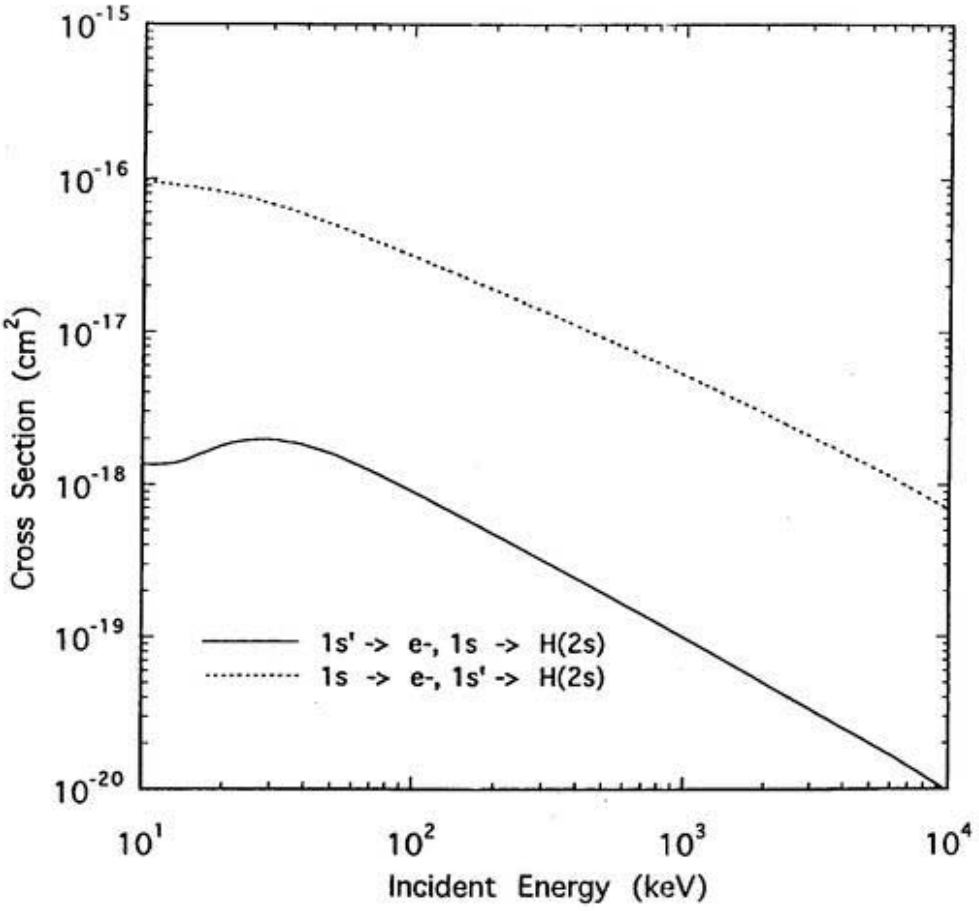

Figure 3.5: Calculated partial cross sections for formation of the excited hydrogen atom, $H^0(2s)$. The solid-curve represents those accompanied with the loosely bound 1s' electron detached and the dotted-curve those accompanied with the tightly bound 1s electron detached.

$$H^- + He(0) \quad \rightarrow \quad H^0(2p) + e^- + \sum_{n'} He(n')$$

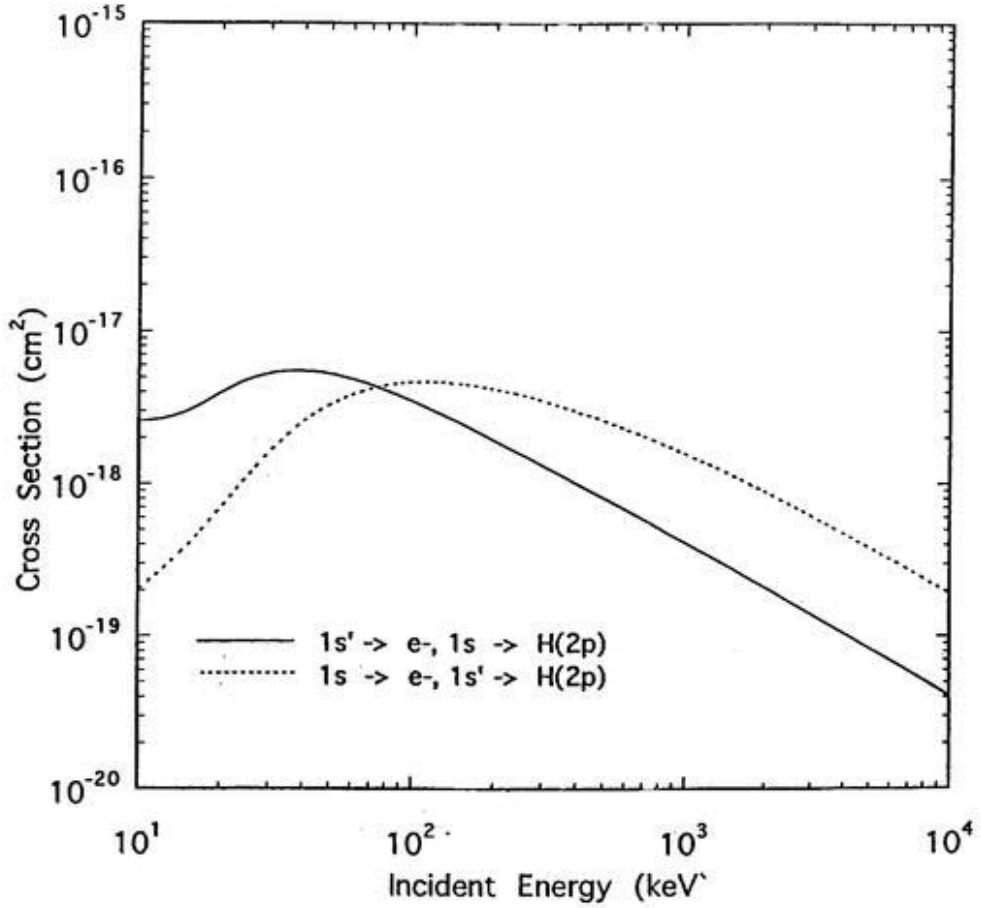

Figure 3.6: Calculated partial cross sections for formation of the excited hydrogen atom, $H^0(2p)$. The solid-curve represents those accompanied with the loosely bound 1s' electron detached and the dotted-curve those accompanied with the tightly bound 1s electron detached and hydrogen atom.

$$H^- + He(0) \quad \rightarrow \quad H^0(1s + 2s + 2p) + e^- + \sum_{n'} He(n')$$

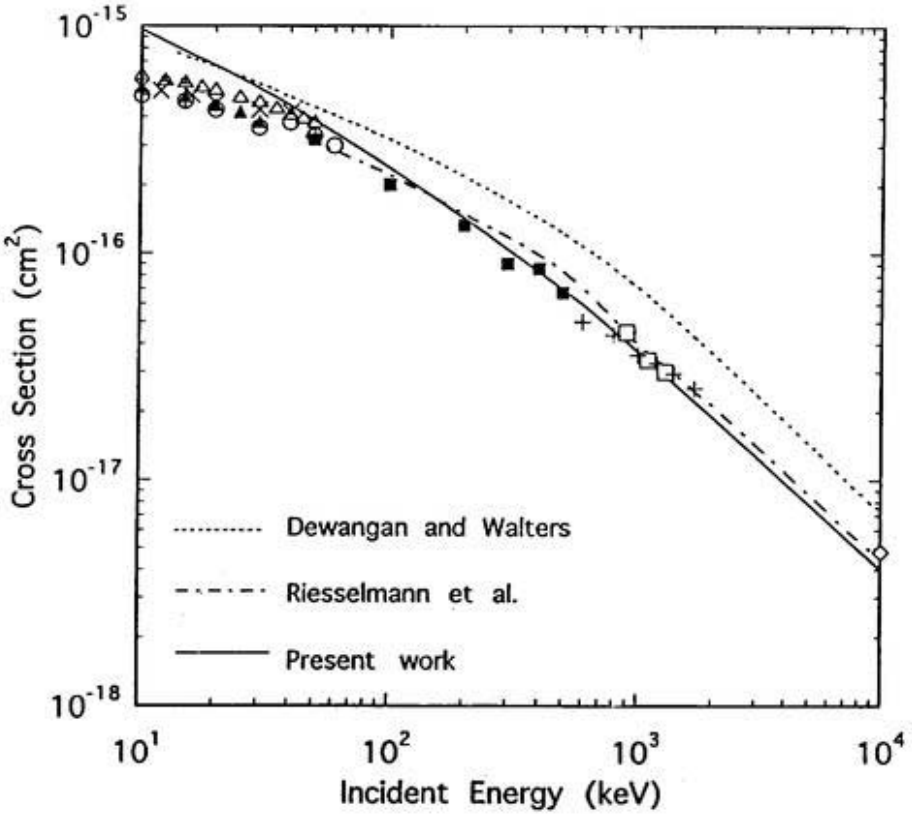

Figure 3.7: Comparison of calculated total single electron detachment cross sections with experimental data in H^- + He collisions. The symbols represent experimental data and are taken from Almeida *et al.* (plus), Anderson *et al.* (solid circle), Berkner *et al.* (open square), Dimov and Dudnikov (solid triangle), Heinemeier *et al.* (solid square), Kvale *et al.* (open triangle), Simpson and Gilbody (diamond), Stier and Barnett (cross) and Williams (open circle). The dotted-curve represents the calculated results of Dewangan and Walters, the dashed-curve those of Riesselmann *et al.* and the solid-curve the present results.

$$H^- + H(0) \quad \rightarrow \quad H^0(1s, 2s \text{ and } 2p) + e^- + \sum_{n'} H(n')$$

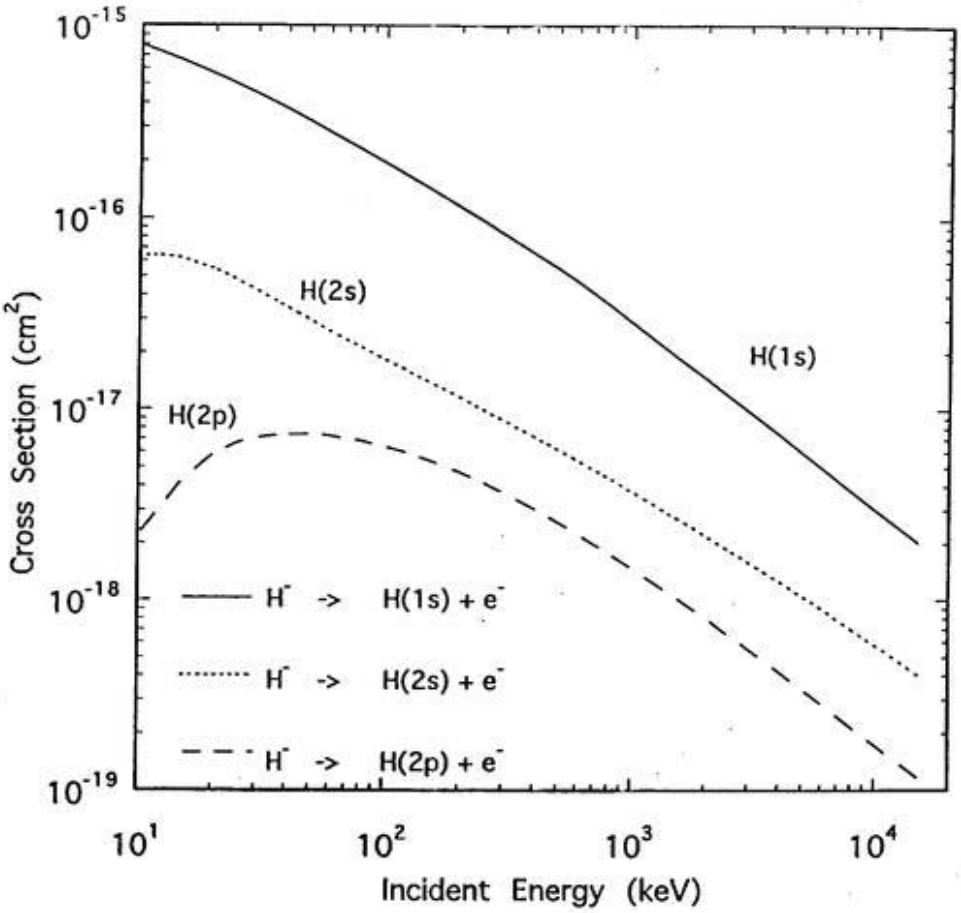

Figure 3.8: Partial cross sections of single electron detachment processes from H^- ions in formation of hydrogen atom target in the ground state, $H^0(1s)$ and the excited states, $H^0(2s)$ and $H^0(2p)$. The solid-curve represents the calculated cross sections for production of hydrogen atom in the ground state $H^0(1s)$, the dotted-curve those for the excited 2s state $H^0(2s)$ and the dashed-curve those for the excited 2p state $H^0(2p)$.

$$H^- + H(0) \quad \rightarrow \quad H^0(1s) + e^- + \sum_{n'} H(n')$$

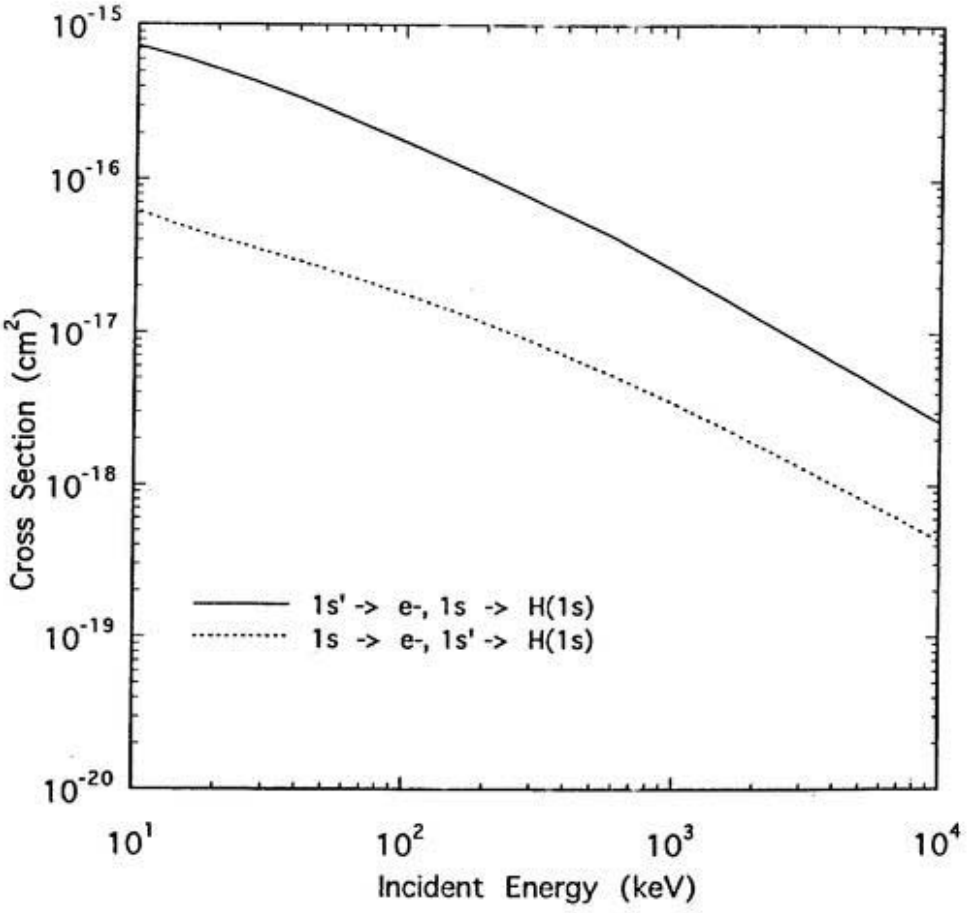

Figure 3.9: Calculated partial cross sections resulting in formation of the ground state of hydrogen atom $H^0(1s)$ in the exit channel. The solid-curve represents those with the loosely bound 1s' electron detached and the dotted-curve those accompanied with the tightly bound 1s electron detached.

$$H^- + H(0) \quad \rightarrow \quad H^0(2s) + e^- + \sum_{n'} H(n')$$

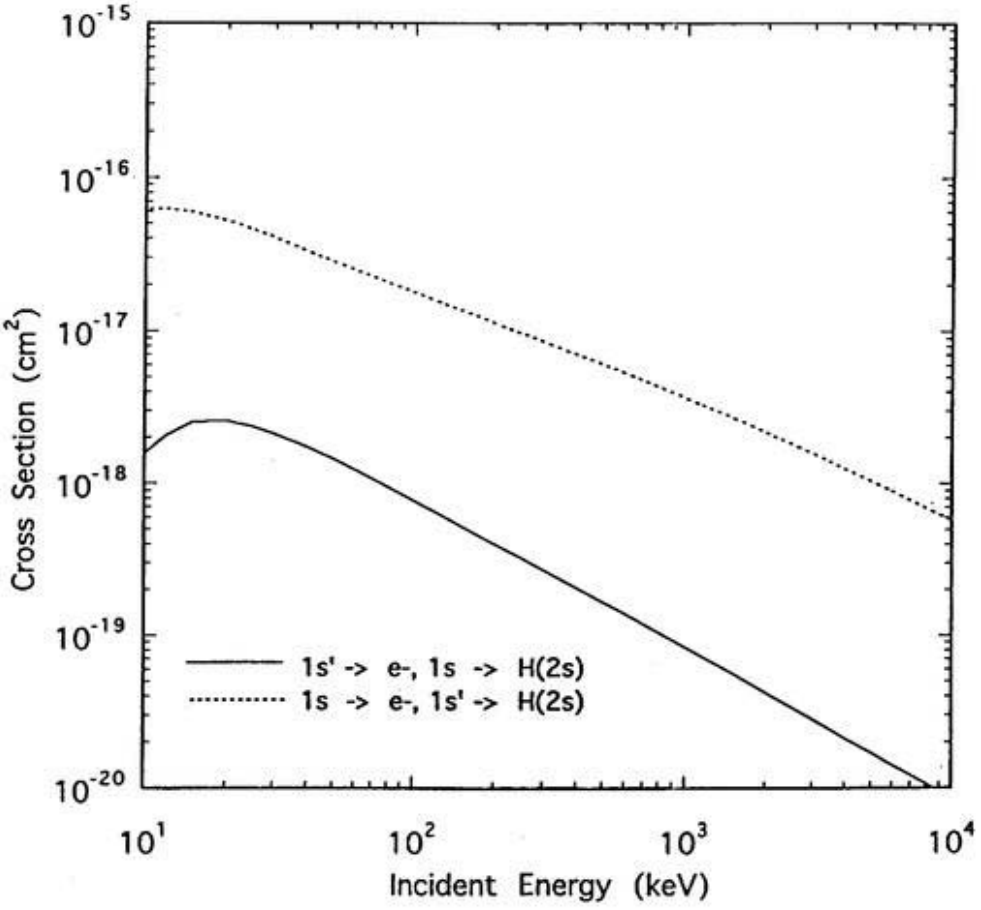

Figure 3.10: Calculated partial cross sections resulting in formation of the excited state hydrogen atom, $H^0(2s)$. The solid-curve represents those with the loosely bound 1s' electron detached and the dotted-curve those with the tightly bound 1s electron detached.

$$H^- + H(0) \quad \rightarrow \quad H^0(2p) + e^- + \sum_{n'} H(n')$$

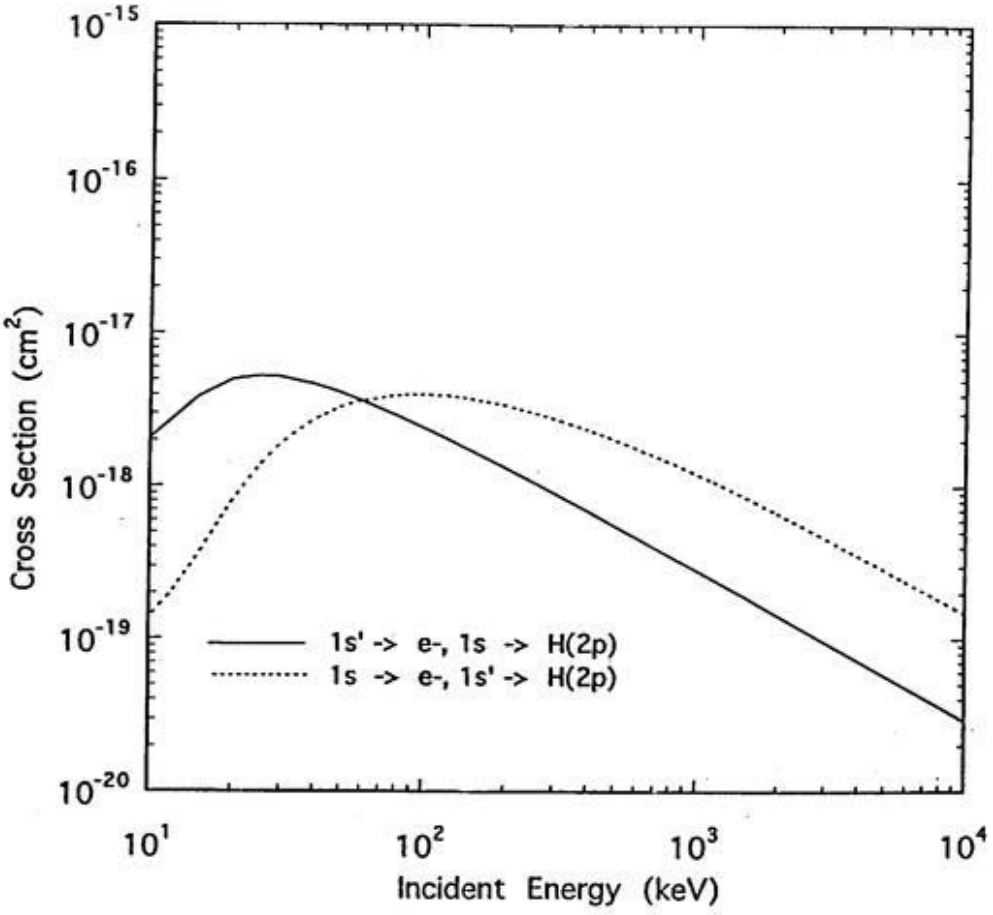

Figure 3.11: Calculated partial cross sections resulting in formation of the excited states of hydrogen atom, $H^0(2p)$. The solid-curve represents those with the loosely bound 1s' electron detached and the dotted-curve those for the tightly bound 1s electron detached.

$$H^- + H(0) \quad \rightarrow \quad H^0(1s + 2s + 2p) + e^- + \sum_{n'} H(n')$$

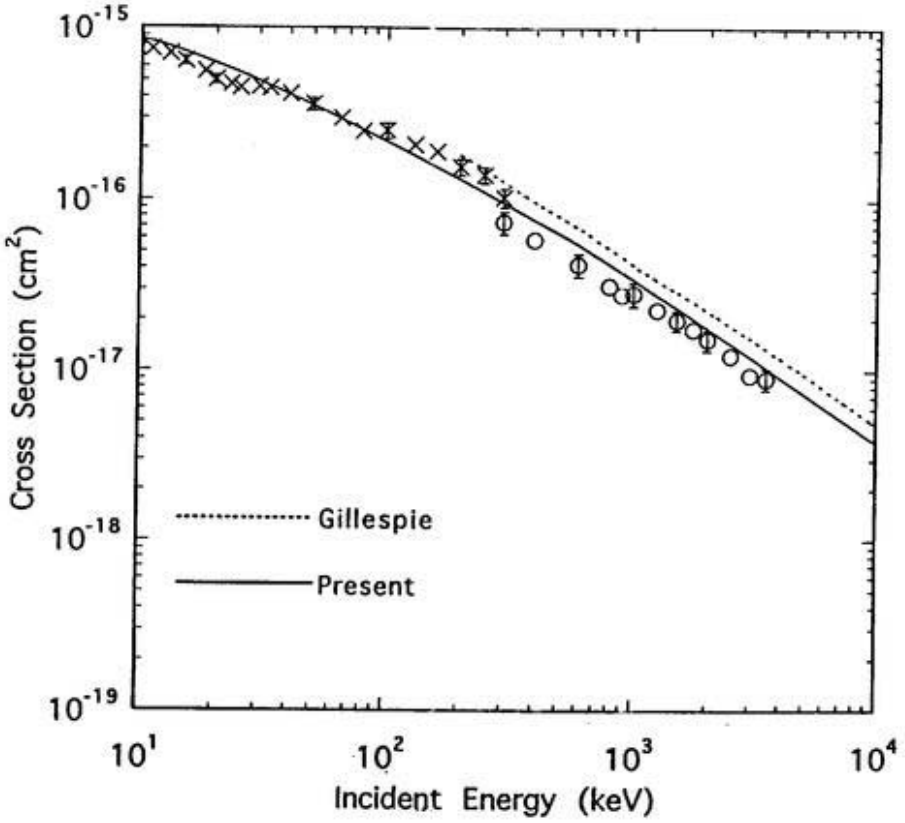

Figure 3.12: Comparison of calculated total single electron detachment cross sections with experimental data in H^- + H collisions. The symbols represent experimental data and are taken from Geddes *et al.* (cross) and Hvelplund and Andersen (open circle) and the solid-curve the present results. The dotted-curve represents the calculated results of Gillespie.

References

Abramowitz M and Stegun I A, 1970 *Handbook of Mathematical Functions*, Dover Publications, Inc., New York

Almeida D P, de Castro Faria N V, Freire, Jr F L, Montenegro E C and de Pinho A G, 1987 Phys. Rev. **A36**, 16

Anderson C J, Girnius R J, Howald A M and Anderson L W, 1980 Phys. Rev. A **22**, 822

Anholt R, 1986 Phys. Lett. **114A**, 126

Bates D R and Walker J C G, 1967 Proc. Phys. Soc. **90**, 333

Belkić Dž, 1984 J. Phys. B **17**, 3629

Belkić Dž and Gayet R, 1975 J. Phys. B **8**, 442

Bethe H A and Jackiw R, 1968 *Intermediate Quantum Mechanics*, Benjamin, New York

Berkner K H, Kaplan S N and Pyle R V, 1964 Phys. Rev. **134**, 1461

Briggs J S and Day M H, 1980 J. Phys. B **13**, 4797

Briggs J S and Drepper F, 1978 J. Phys. B **11**, 1033

Day M H, 1981 J. Phys. B **14**, 231

Dimov G I and Dudnikov V G, 1967 Sov. Phys.-Tech. Phys. **11**, 919

Dewangan D P and Walters H R J, 1978 J. Phys. B **11**, 3983

Dmitriev I S and Nikolaev V S, 1963 Sov. Phys.-JETP **17**, 447

Drukarev G F, 1970 Sov. Phys.-JETP **31**, 1193

Geddes J, Hill J and Gilbody H B, 1981 J. Phys. B **14**, 4837

Geddes J, Hill J, Shah M B, Goffe T V and H B Gilbody, 1980 J. Phys. B **13**, 319

Gillespie G H, 1977 Phys. Rev. **15**, 563

Gradshteyn I S and Ryzhik I M, 1994 *Table of Integrals, Series and Productions*

Fifth Edition, Academic Press, San Diego, New York, Boston, London, Sydney, Tokyo, Toronto

Harnois M, Falk R A, Geballe R and Risley J, 1977 Phys. Rev. A **16**. 2256

Hartley D P and Walters W E, 1987 J. Phys. B **20**, 1938

Hvelplund P and Andersen A, 1982 Phys. Scr. **26**, 370

Heinemeier J, Hvelplund P and Simpson F R, 1976 J. Phys. B **9**, 2669

Kaminsky A K, Myakishev N G and Popova M I, 1980 J. Phys. B**13**, 1161

Kvale D P, Allen J S, Fang X D, Sen A and Matulioniene R, 1995 Phys. Rev. A **51**, 1351

Levy II H, 1969 Phys. Rev. **185**, 7

Lodge J G, 1969 J. Phys. B. **2**, 322

McGuire J H, Stolterfoht N and Simony P R, 1981 Phys. Rev. A **24**, 97

Montenegro E C and Meyerhof W E, 1991 Phys. Rev. A **43**, 2289

Montenegro E C, Meyerhof W E and McGuire J H, 1994 Adv. At. Mol. Opt. Phys **34**, 249

Orbeli A L, Andreev E P, Ankudinov V A and Dukel'skii V M, 1970 Sov. Phys.-JETP **31**, 1044

Rule D W, 1977 Phys. Rev. **16**, 19

Radchenko V I and Ved'manov G D, 1995 JETP **80**, 670

Riesselmann K, Anderson L W, Durand L and Anderson C J, 1991 Phys. Rev. A **43**, 5934

Risley J S, de Heer F J and Kerkdijk C B, 1978 J. Phys. B **11**, 1783

Simpson F R and Gilbody H B, 1972 J. Phys. B **5**, 1959

Shull H and Löwdin P-O, 1956 J. Chem. Phys. **25**, 1035

Stier P M and Barnett C F, 1956 Phys. Rev. **103**, 896

Tawara H and Russek A, 1973 Rev. Mod. Phys. **45**, 178

Victor G A, Phys. Rev **184**, 43

Williams J F, 1967 Phys. Rev. **154**, 9

4 Single electron detachment from H^- ions in collisions with bare positive ions

4.1 Outline of present theory

In this section, we consider the electron detachment processes of H^- ions in collisions with bare positive ions with the charge Z, A^{Z+}, where strong Coulomb interactions may play a role,

$$A^{Z+} + H^- \quad \rightarrow \quad A^{Z+} + H^0(1s \text{ and } 2s) + e^-. \tag{4.1}$$

It is assumed that the electron capture into positive ions from H^- ions is negligible at the present energy.

In order to describe the distortion effects in atom-ion or ion-ion collisions, the Continuum Distorted Wave (CDW) method is widely used for calculations of cross sections (see, for example, Cheshire 1964, Dodd and Greider 1966, Gayet 1972, Belkić and Janev 1973, Belkić 1977, Belkić 1978). And the Eikonal Initial State (EIS) method is used for the distorted wave in the entrance channel in the CDW approximation (CDW-EIS approximation, Crothers and McCann 1983, Fainstein *et al.* 1990, Fainstein *et al.* 1991).

The present collision system consists of four particles, namely two electrons and two nuclei. The 4-Body CDW method was introduced by Belkić and Mančev (1992) and in some calculations was used the 4-Body CDW or 4-Body CDW-EIS method (Belkić and Mančev 1993, Belkić 1996, Gayet *et al.* 1996, Belkić 1997a, Belkić 1997b, Belkić *et al.* 1997) in four particle collision system.

Here we use the 4-Body CDW-EIS method to investigate the collision process shown in (4.1). The process (4.1) was treated by Belkić (1996 and 1997) based

on the 4-Body distorted scattering theory using the plane wave for the detached electron wave function. In the present calculations, we take the plane wave for the detached electron wave function which includes the effect of the Coulomb field in H^- ions (see Sec.2.2).

The coordinate of this collision system is shown in Fig. 4.1 and Fig. 4.2 : $\boldsymbol{x}_1$ and $\boldsymbol{x}_2$ are the electron coordinates from proton in H^- ion, $\boldsymbol{s}_1$ and $\boldsymbol{s}_2$ the electron coordinates from positive ion, $\boldsymbol{r}_a$ the positive ion coordinate from the center-of-mass in H^- ion system in the entrance channel, $\boldsymbol{r}_b$ the positive ion coordinate from the center-of-mass for neutral hydrogen atom and the detached electron system in the exit channel:

$$\boldsymbol{r}_a = \frac{1}{2}\frac{M_p}{M_p+2}(\boldsymbol{x}_1+\boldsymbol{x}_2) - \frac{1}{2}(\boldsymbol{s}_1-\boldsymbol{s}_2) \tag{4.2}$$

$$\boldsymbol{r}_b = \frac{1}{2}\frac{M_t}{M_t+2}(\boldsymbol{s}_1+\boldsymbol{s}_2) - \frac{1}{2}(\boldsymbol{x}_1-\boldsymbol{x}_2) \tag{4.3}$$

where M_p is the mass of the incident positive ion and M_t the mass of proton in atomic units.

4.2 Calculations

The total Hamiltonian for reaction (1.1) in the entrance channel is given as follows:

$$H = K_a + H_i \tag{4.4}$$

$$K_a = -\frac{\nabla^2_{\boldsymbol{r}_a}}{2M} \tag{4.5}$$

$$H_i = H_a + V_a \tag{4.6}$$

$$H_a = -\frac{\nabla^2_{\boldsymbol{x}_1}}{2m} - \frac{\nabla^2_{\boldsymbol{x}_2}}{2m} - \frac{1}{x_1} - \frac{1}{x_2} + \frac{1}{r_{12}} \tag{4.7}$$

$$V_a = \frac{Z}{R} - \frac{Z}{s_1} - \frac{Z}{s_2} \tag{4.8}$$

where K_a is the kinetic energy of total system in the entrance channel, H_a the Hamiltonian of H^- ion system, V_a the perturbation term between positive ion and H^- ion, M the reduced-mass of the total system, m the reduced-mass of H^- ion system:

$$M = \frac{M_p(M_t+2)}{M_p+M_t+2}$$

$$m = \frac{M_t+1}{M_t+2}$$

and r_{12} the distance between two electrons,

$$r_{12} = |\boldsymbol{x}_1 - \boldsymbol{x}_2| = |\boldsymbol{s}_1 - \boldsymbol{s}_2|. \tag{4.9}$$

On the other hand, the total Hamiltonian for reaction (4.1) in the exit channel is given as follows:

$$H = K_b + H_f \tag{4.10}$$

$$K_b = -\frac{\nabla^2_{\boldsymbol{r}_b}}{2M} \tag{4.11}$$

$$H_f = H_b + V_b \tag{4.12}$$

$$H_b = -\frac{\nabla^2_{\boldsymbol{x}_1}}{2m} - \frac{\nabla^2_{\boldsymbol{x}_2}}{2m} - \frac{1}{x_1} \tag{4.13}$$

$$V_b = \frac{Z}{R} - \frac{1}{x_2} - \frac{Z}{s_1} - \frac{Z}{s_2} + \frac{1}{r_{12}} \tag{4.14}$$

where K_b is the kinetic energy of total system in the exit channel, H_b the Hamiltonian of neutral hydrogen atom system and the kinetic energy of the detached electron in the exit channel, V_b the perturbation term among neutral hydrogen atom, the

detached electron and positive ion in the exit channel.

Firstly, we consider the wave function in the entrance channel. We take the undistorted wave function in the entrance as follows:

$$\phi_a = \Phi_{H^-}(\boldsymbol{x}_1, \boldsymbol{x}_2) e^{-iE_a t}, \tag{4.15}$$

where Φ_{H^-} is the wave function of H^- ion which is defined in Sec.2.1 and E_a the corresponding energy of H^- ion. Then Eqs. (4.7) and (4.15) satisfy the following Schrödinger equations:

$$(H_i - i\frac{\partial}{\partial t})|\phi_a\rangle = 0 \tag{4.16}$$

$$(H_a - E_a)|\Phi_{H^-}\rangle = 0. \tag{4.17}$$

Now we must define the distorted wave function in the entrance channel. The asymptotic behavior of the perturbative potential in the initial conditions is

$$t \to -\infty, \quad V_a = \frac{Z(Z_{H^-} - 2)}{R}. \tag{4.18}$$

And the wave function in the asymptotic condition ($t \to -\infty$) is given as follows:

$$\Psi^+ = \phi_a e^{-i\nu_a ln(vR - \boldsymbol{v}\cdot\boldsymbol{R})} \tag{4.19}$$

where

$$\nu_a = \frac{Z(Z_{H^-} - 2)}{v}. \tag{4.20}$$

Equation (4.19) includes the long range interaction between positive ion with nuclear charge Z and electrons in H^- ion and the interaction of the inter-nucleus. So, the $\phi_a e^{-i\nu_a ln(vR - \boldsymbol{v}\cdot\boldsymbol{R})}$ is based on the Eikonal Initial State (EIS) approximation which was introduced by Crothers and McCann (1983).

Here we choose the distortion effect of the interaction between a detaching electron at $\boldsymbol{x}_1$ and the positive ion because in the present calculations the detachment of another electron at $\boldsymbol{x}_2$ is not treated. Then, Eq. (4.19) can be rewritten as follows:

$$\Psi^+ = \phi_a e^{-i\nu_{a'} ln(vs_1+\boldsymbol{v}\cdot\boldsymbol{s}_1)} e^{-i\nu_{a''} ln(vR-\boldsymbol{v}\cdot\boldsymbol{R})} \tag{4.21}$$

$$\nu_{a'} = \frac{Z}{v}, \quad \nu_{a''} = \frac{Z(Z_{H^-}-1)}{v}, \tag{4.22}$$

where Z is the charge of positive ion, Z_{H^-} the charge of H^- ion, and v the incident velocity of this collision system.

The distorted potential satisfies the conditions of Eqs. (4.16) and (4.17) as follows:

$$(H_i - i\frac{\partial}{\partial t})|\Psi^+\rangle = V_{d_a}|\Psi^+\rangle \tag{4.23}$$

where V_{d_a} is the distorted potential in the entrance channel. Equation (4.23) leads to the following form (see Appendix B)

$$\begin{aligned} V_{d_a}\Psi^+ = \phi_a\{ & -\frac{1}{2}\nabla^2_{\boldsymbol{x}_1} e^{-i\nu_{a'} ln(vs_1+\boldsymbol{v}\cdot\boldsymbol{s}_1)} e^{-i\nu_{a''} ln(vR-\boldsymbol{v}\cdot\boldsymbol{R})} \\ & -\nabla_{\boldsymbol{x}_1}\phi_a \cdot \nabla_{\boldsymbol{s}_1} e^{-i\nu_{a'} ln(vs_1-\boldsymbol{v}\cdot\boldsymbol{x}_1)} e^{-i\nu_{a''} ln(vR-\boldsymbol{v}\cdot\boldsymbol{R})} \\ & +(\frac{Z}{R}-\frac{Z}{s_2})\}\Psi^+ \end{aligned} \tag{4.24}$$

and the distorted potential is given as follows:

$$\begin{aligned} V_{d_a} = & \frac{1}{s_1}\frac{\nu_{a'}}{vs_1+\boldsymbol{v}\cdot\boldsymbol{s}_1} - \nabla_{\boldsymbol{x}_1} ln\phi_a \cdot \nabla_{\boldsymbol{s}_1} \\ & +(\frac{Z}{R}-\frac{Z}{s_2}). \end{aligned} \tag{4.25}$$

Z_{H^-} is equivalent to proton in the present collision system (4.1), namely

$$Z_{H^-} = 1$$

$$e^{-i\nu_{a''} ln(vR-\boldsymbol{v}\cdot\boldsymbol{R})} = 1.$$

The final form of the wave function in the asymptotic condition of the entrance channel is

$$\Psi^+ = \phi_a e^{-i\nu_{a'} ln(vs_1 + \boldsymbol{v}\cdot\boldsymbol{s}_1)}. \tag{4.26}$$

Secondly, we consider the wave function in the exit channel. We take the undistorted wave function in the exit channel as follows:

$$\phi_b = \Phi_{H^0(nlm),e^-_{Z(j)}} e^{-iE_b t} e^{-iE_e t}, \tag{4.27}$$

where E_b is the corresponding energy of H^0(nlm) atom, E_e the kinetic energy of the detached electron ($e^-_{Z(j)}$) and $\phi_{H^0(nlm),e^-_{Z(j)}}$ the wave function representing H^0(nlm) atom and the detached electron which is defined in Sec.2.2. Here as we do not treat the electron detachment process of another electron at coordinate $\boldsymbol{x}_2$, the form of the wave function is given as follows:

$$\Phi_{H^0(nlm),e^-_{Z(j)}}(\boldsymbol{x}_1, \boldsymbol{x}_2) = N_f \phi_{e^-_{Z(j)}}(\boldsymbol{x}_1)\phi_{H^0(nlm)}(\boldsymbol{x}_2). \tag{4.28}$$

Then Eqs. (4.13) and (4.27) satisfy the following Schrödinger equations:

$$(H_f - i\frac{\partial}{\partial t})|\phi_b\rangle = 0 \tag{4.29}$$

$$(H_b - E_b - E_e)|\phi_{H^0(nlm),e^-_{Z(j)}}\rangle = 0. \tag{4.30}$$

Now, we define the distorted wave function in the exit channel. The asymptotic behavior of the perturbative potential in the final conditions is

$$t \to +\infty, \quad V_a = -\frac{Z}{s_1} + \frac{Z(Z_{H^-} - 1)}{R}. \tag{4.31}$$

And the wave function in the exit channel is

$$\Psi^- = \phi_b e^{\pi\nu_{b'}} \Gamma(1 + i\nu_{b'})_1 F_1(-i\nu_{b'}, 1, -ips_1 - i\boldsymbol{p}\cdot\boldsymbol{s}_1) e^{-i\nu_{b''} ln(vR + \boldsymbol{v}\cdot\boldsymbol{R})} \tag{4.32}$$

$$\nu_{b'} = \frac{Z}{p}, \quad \nu_{b''} = \frac{Z(Z_{H^-} - 1)}{v}. \tag{4.33}$$

The distorted potential in Eq. (4.32) satisfies the conditions of Eqs. (4.29) and (4.30):

$$(H_f - i\frac{\partial}{\partial t})|\Psi^-\rangle = V_{d_b}|\Psi^-\rangle. \tag{4.34}$$

Equation (4.34) leads to the following form (see Appendix C)

$$V_{d_b}\Psi^- = (\frac{Z}{R} - \frac{Z}{s_2} + \frac{1}{r_{12}} - \frac{1}{x_1})\Psi^-, \tag{4.35}$$

and, finally, the distorted potential is given as follows:

$$V_{d_b} = (\frac{Z}{R} - \frac{Z}{s_2}) + (\frac{1}{r_{12}} - \frac{1}{x_1}) \tag{4.36}$$

(see Appendix C). Z_{H^-} is equivalent to proton in the present collision system, namely

$$\begin{aligned} Z_{H^-} &= 1 \\ e^{-i\nu_a \ln(vR - \boldsymbol{v}\cdot\boldsymbol{R})} &= 1. \end{aligned}$$

Thus, the final form of the distorted wave can be rewritten as:

$$\Psi^- = \phi_b e^{-i\nu_b} e^{\pi\nu_b} \Gamma(1 + i\nu_b)\, {}_1F_1(-i\nu_b, 1, -ips_1 - i\boldsymbol{p}\cdot\boldsymbol{s}_1). \tag{4.37}$$

Using the distorted potentials V_{d_a} and V_{d_b}, and the distorted wave functions Ψ^+ and Ψ^-, the transition amplitudes in 'prior' and 'post' form lead to the following forms:

$$P_{prior} = \langle\Psi^-|V_{d_a}|\Psi^+\rangle \tag{4.38}$$

$$P_{post} = \langle\Psi^+|V_{d_b}|\Psi^-\rangle^\dagger, \tag{4.39}$$

(† represents the complex conjugate inversion). These transition amplitudes can be written as

$$
\begin{aligned}
P_{prior} = \quad & \int\int\int ds_1 d\boldsymbol{x}_1 d\boldsymbol{x}_2 \\
& \times \; e^{i\boldsymbol{q}\cdot\boldsymbol{r}_a}\phi^*_{e^-_{Z(j)}}(\boldsymbol{x}_1)\phi^*_{H^0(nlm)}(\boldsymbol{x}_2)N(b')\,{}_1F_1(-i\nu_{b'},1,-ips_1-i\boldsymbol{p}\cdot\boldsymbol{s}_1) \\
& + \; \{\frac{1}{2}\nabla^2_{\boldsymbol{s}_1}e^{-i\nu_{a'}ln(vs_1+\boldsymbol{v}\cdot\boldsymbol{s}_1)}\Phi_{H^-}(\boldsymbol{x}_1,\boldsymbol{x}_2) \\
& + \; \nabla_{\boldsymbol{x}_1}\Phi_{H^-}(\boldsymbol{x}_1,\boldsymbol{x}_2)\cdot\nabla_{\boldsymbol{s}_1}e^{-i\nu_{a'}ln(vs_1+\boldsymbol{v}\cdot\boldsymbol{s}_1)} \\
& + \; (\frac{Z}{s_1}-\frac{Z}{R})e^{-i\nu_{a'}ln(vs_1+\boldsymbol{v}\cdot\boldsymbol{s}_1)}\Phi_{H^-}(\boldsymbol{x}_1,\boldsymbol{x}_2)\}
\end{aligned}
\tag{4.40}
$$

and

$$
\begin{aligned}
P_{post} = \quad & \int\int\int ds_1 d\boldsymbol{x}_1 d\boldsymbol{x}_2 \\
& \times \; e^{i\boldsymbol{q}\cdot\boldsymbol{r}_a}\phi^*_{e^-_{Z(j)}}(\boldsymbol{x}_1)\phi^*_{H^0(nlm)}(\boldsymbol{x}_2)N(b')\,{}_1F_1(-i\nu_{b'},1,-ips_1-i\boldsymbol{p}\cdot\boldsymbol{s}_1) \\
& + \; \{(\frac{Z}{s_1}-\frac{Z}{R})e^{-i\nu_{a'}ln(vs_1+\boldsymbol{v}\cdot\boldsymbol{s}_1)}\Phi_{H^-}(\boldsymbol{x}_1,\boldsymbol{x}_2) \\
& + \; (\frac{1}{r_{12}}-\frac{1}{R})e^{-i\nu_{a'}ln(vs_1+\boldsymbol{v}\cdot\boldsymbol{s}_1)}\Phi_{H^-}(\boldsymbol{x}_1,\boldsymbol{x}_2)\}
\end{aligned}
\tag{4.41}
$$

(Belkić 1977, McDowell and Coleman 1970), where $N(b')$ is the normalization factor in the exit channel given as;

$$N(b') = e^{\pi\nu_{b'}}\Gamma(1+i\nu_{b'}) \tag{4.42}$$

and $\boldsymbol{q}$ the momentum transfer given as follows:

$$\boldsymbol{q} = -\boldsymbol{\eta} - \frac{\Delta E}{v^2}v. \tag{4.43}$$

Here v is the incident velocity, ΔE the internal energy change between the entrance channel and the exit channel,

$$\Delta E = E_{H^-} - E_{H^0(nlm)} - E_{e^-}$$

where E_{H^-} : the eigenenergy of H^- ion

$E_{H^0(nlm)}$: the eigenenergy of H^0(nlm) atom

$E_{H^0(nlm)}$: the kinetic energy of the detached electron

and $\boldsymbol{\eta}$ the transversal component of the momentum transfer, $\boldsymbol{q}$, which has the following relation:

$$\boldsymbol{\eta} \cdot \boldsymbol{v} = 0. \tag{4.44}$$

In the present calculations the last two terms in Eqs. (4.40) and (4.41) vanish because $\boldsymbol{x_1} \ll \boldsymbol{s_1}$ and $\boldsymbol{s_1} \approx \boldsymbol{R}$.

Finally the corresponding cross sections are given as follows:

$$\sigma_{prior} = \int d\boldsymbol{\kappa} \int d\boldsymbol{\eta} |\frac{P_{prior}(\boldsymbol{\eta})}{2\pi v^2}|^2 \tag{4.45}$$

$$\sigma_{post} = \int d\boldsymbol{\kappa} \int d\boldsymbol{\eta} |\frac{P_{post}(\boldsymbol{\eta})}{2\pi v^2}|^2. \tag{4.46}$$

In the present work, we calculate the cross sections using only the 'prior' form of Eq. (4.45).

4.3 Results and discussion

In this section, we show the calculated results of total and partial cross sections for electron detachment process (4.1) and compare them with experimental data available.

Firstly, we calculate the cross sections for electron detachment of H^- ions in collisions with protons:

$$H^+ + H^- \quad \rightarrow \quad H^+ + H^0(1s \text{ and } 2s) + e^-. \tag{4.47}$$

Numerical cross sections data calculated are given in Appendix D.3.

Figure 4.3 shows the calculated partial cross section for process (4.47). The solid line denotes those for production of the ground state neutral hydrogen atoms, $H^0(1s)$, in the exit channel and the dotted line those of the excited state neutral hydrogen atoms, $H^0(2s)$. The cross sections of production of $H^0(1s)$ is far larger (more than two orders of magnitude) than those of $H^0(2s)$ in all the energies investigated. This feature of cross sections is similar to that in collisions with neutral atoms mentioned in Sec. 3. However, ratios of production of the ground state $H^0(1s)$ to that of the excited state $H^0(2s)$ are very much different from collisions with protons and with neutral atoms. This difference can be understood as follows: In Eq. (4.40), interactions between proton and the remaining electron disappear in the asymptotic condition. It should be noted, however, that the cross sections for production of the excited state hydrogen atoms $H^0(2p)$ become zero because the direct transitions of the ground state (Hylleraas-Eckart function) to the excited 2p state (neutral hydrogen atom wave function) included in Eq. (4.40) vanish. The hydrogen like wave function of the 2p state includes the orbital angular momentum component. On the other hand, the Hylleraas-Eckart function does not include the orbital angular momentum component. Therefore, the transition amplitude becomes zero in integration in Eq. (4.40).

Figures 4.4 and 4.5 show the cross sections for production of $H^0(1s)$ and $H^0(2s)$ atoms in the exit channel due to the tightly bound electron (1s) and the loosely

bound electron (1s') detachment processes, respectively. In production of the ground state hydrogen atoms, $H^0(1s)$, the loosely bound 1s' electron detachment process is dominant in all energies. On the other hand, in production of the excited state hydrogen atoms, $H^0(2s)$, the tightly bound 1s electron detachment process is dominant. Surprisingly, the difference of formation of the excited $H^0(2s)$ from the contribution of two (1s and 1s') electrons is huge (more than four orders of magnitude) (see Fig. 4.5).

From the view point of applications to NBI, the present results for proton impact may provide better conditions than those for neutral atoms because of very small fractions of the excited state $H^0(2s)$ atoms. Indeed, the excited state H^0 atoms are easily ionized before reaching the main plasmas to heat them, thus reducing the heating efficiencies.

Now, we compare the calculated results for electron detachment cross sections with experimental data for collisions with protons, namely, process (4.47) and for those with neutral hydrogen atom:

$$H(0) + H^- \quad \rightarrow \quad \sum_{n'} H(n') + H^0(1s, 2s, \text{ and } 2p) + e^-. \qquad (4.48)$$

In Fig. 4.6, the solid-curve represents the calculated results for process (4.47), the dotted-curve those for process (4.48) and the open squares the experimental data (Peart *et al.* 1970) for process (4.47), the solid-triangles the experimental data (Peart *et al.* 1976) in collisions with electrons with the equivalent velocity and the dashed-curve the previous theoretical work (Belkić 1997a and 1997b) for $H^+ + H^-$ collisions. Figure 4.6 indicates that our calculations overestimate the cross sections in all collision energies studied, but in high energy region, our results approach the

experimental data, meanwhile, the calculation results by Belkić is in good agreement with the experimental data. Belkić used the detailed wave function for H^- ion. On the other hand, we used the Hylleraas-Eckart function for H^- ion. Thus, the difference between two calculations may be due to the wave functions used for H^- ion.

Finally, we calculate those for other positive ion (He^{+2} and Li^{+3}) impact.

Numerical cross section data calculated are given in Appendixes D.4 and D.5.

In Fig. 4.7, where the electron detachment cross sections divided by the square of positive ion charge are plotted against the collision energy, the solid-curve denotes those for proton, the dashed-curve those for He^{+2} and the dotted-curve those for Li^{+3} ion impact. The present calculated results suggest that the cross sections of single electron detachment from H^- ions in collisions with various bare positive ions are roughly proportional to the square of positive ion charge, Z, at least in high energy region. So far no experiment has been performed in such positive ion-negative ion collisions at high energy region, except for one preliminary work (Tawara *et al.* 1999).

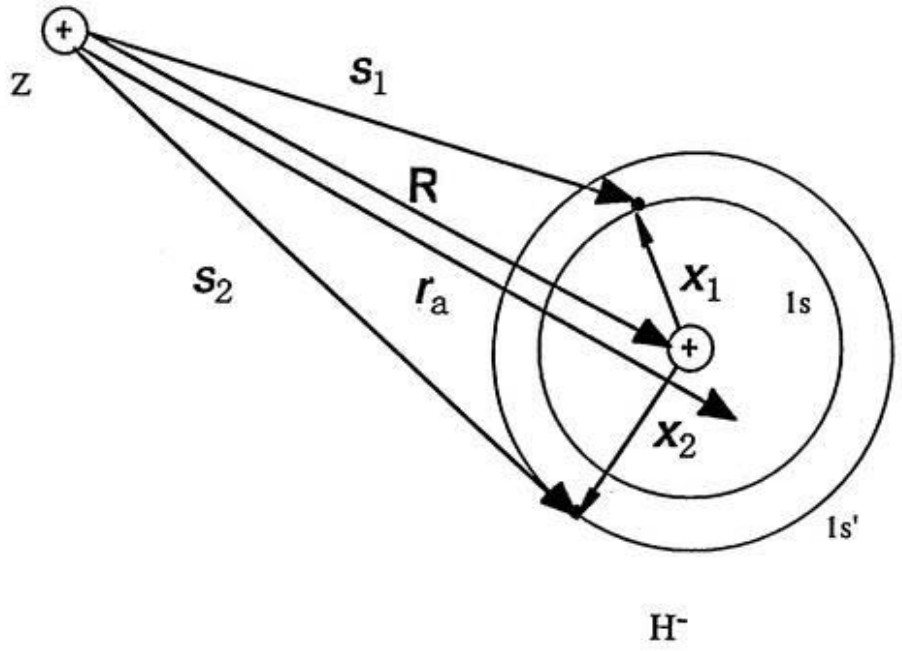

Figure 4.1: Coordinate system of the entrance channel.

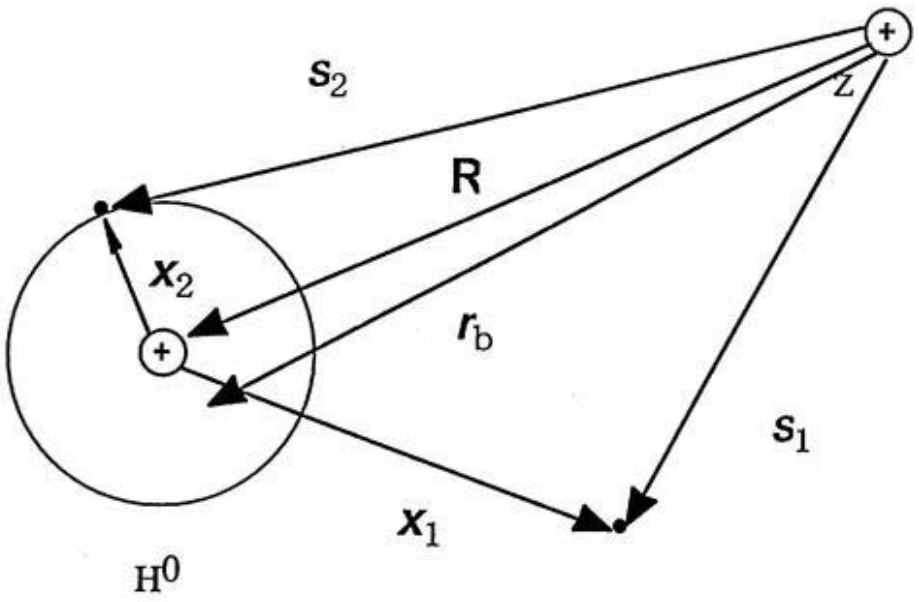

Figure 4.2: Coordinate system of the exit channel.

$$H^+ + H^- \quad \rightarrow \quad H^+ + H^0(1s \text{ and } 2s) + e^-$$

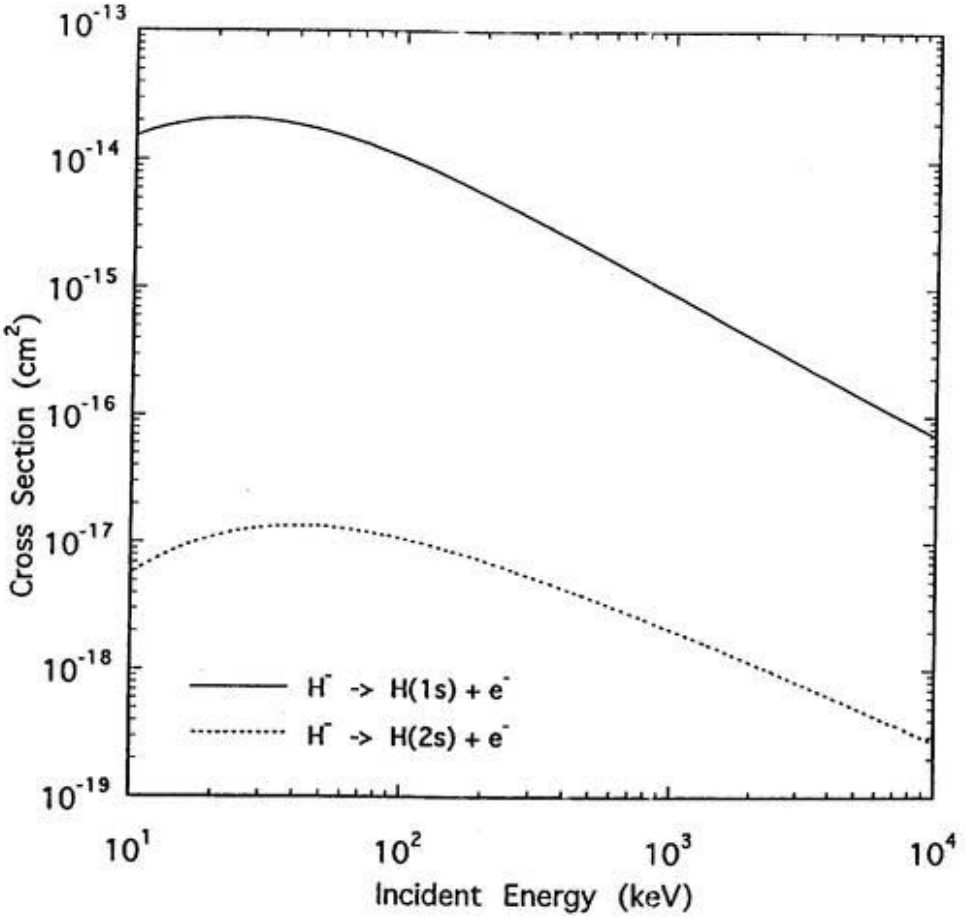

Figure 4.3: Calculated partial cross sections for single electron detachment in $H^+ + H^-$ collisions. The solid and the dotted lines represent those for hydrogen atoms in the ground state $H^0(1s)$, and those for hydrogen atoms in the excited state $H^0(2s)$, respectively.

$$H^+ + H^- \quad \rightarrow \quad H^+ + H^0(1s) + e^-$$

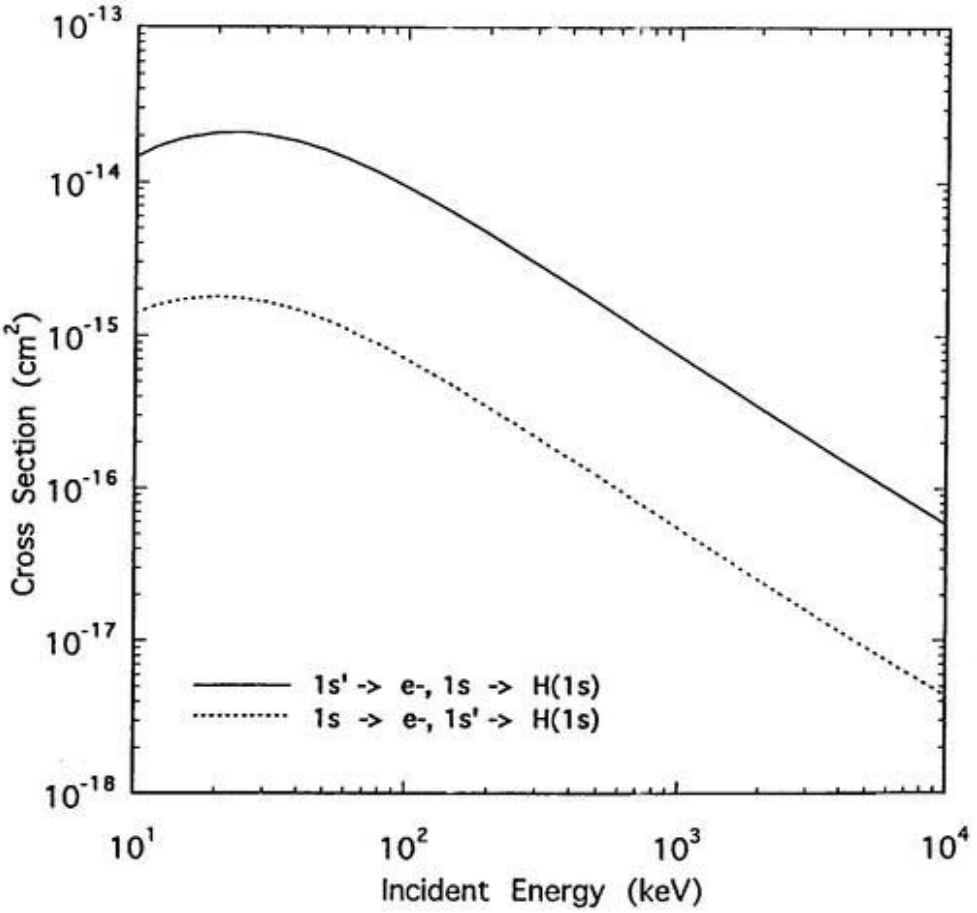

Figure 4.4: Partial cross sections for production of the ground state hydrogen atoms, $H^0(1s)$. The solid line denotes the detachment of the loosely bound (1s') electron and the dotted line the detachment of the tightly bound (1s) electron.

$$H^+ + H^- \quad \rightarrow \quad H^+ + H^0(2s) + e^-$$

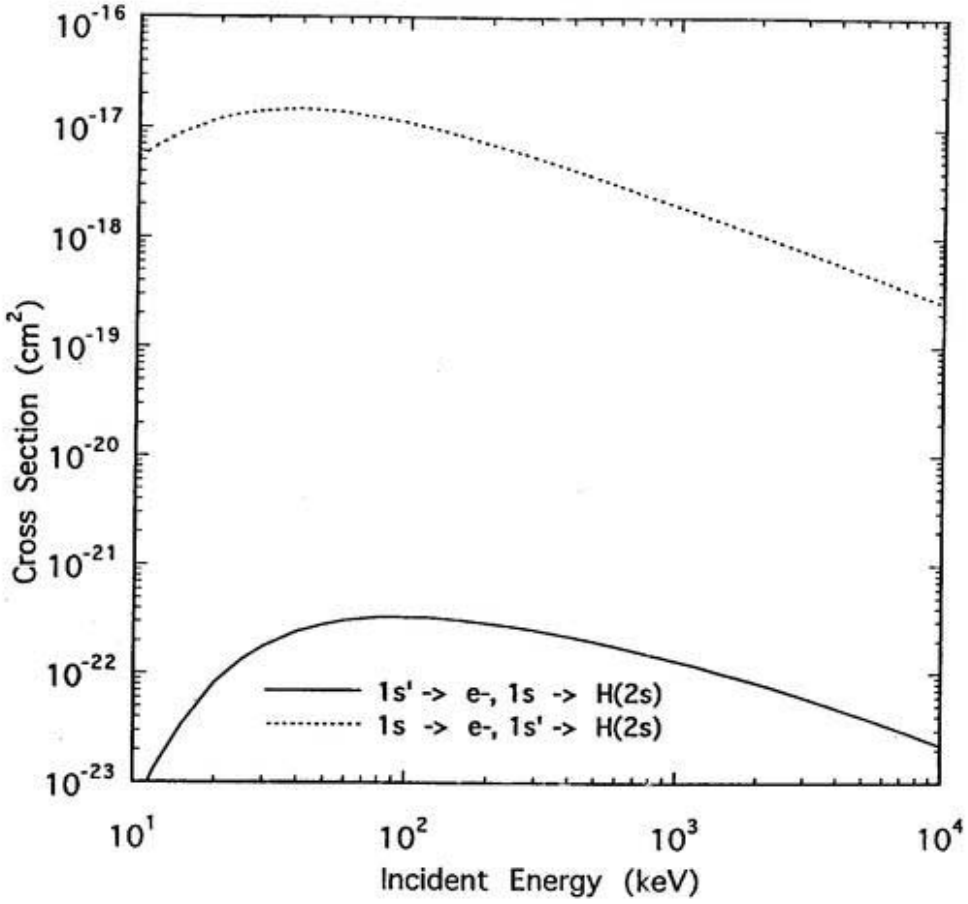

Figure 4.5: Partial cross sections for production of the excited state hydrogen atoms, $H^0(2s)$. The solid line denotes the detachment of the loosely bound (1s') electron and the dotted line the detachment of the tightly bound (1s) electron.

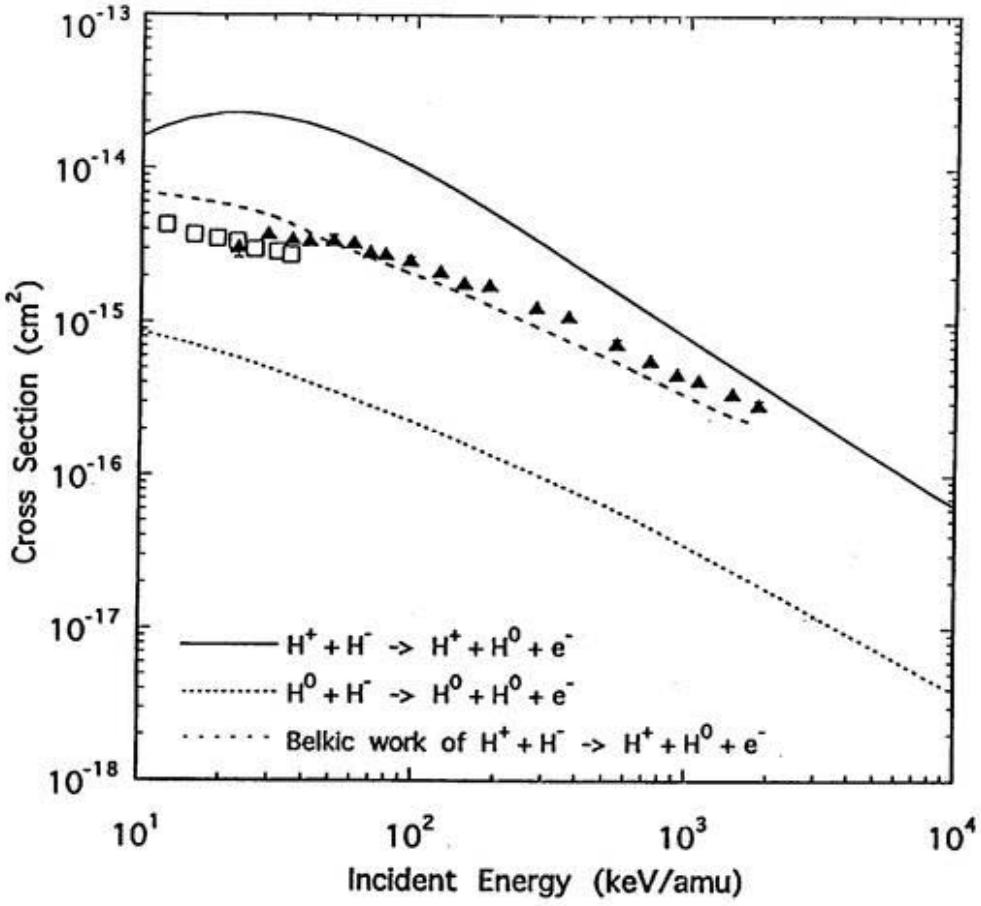

Figure 4.6: Comparison of electron detachment cross sections in $H^+ + H^-$ and $H^0 + H^-$ collisions. Symbols represent the experimental data: solid triangles Peart *et al.* (1976) for $H^+ + H^-$ and open squares Peart *et al.* (1970) for $H^- +$ electron collisions in electron impact with the equivalent velocity. The solid line denotes the present calculated results for $H^+ + H^-$ collisions, the dotted line those for $H + H^-$ collisions and the dashed line those by Belkić's work of (1997) $H^+ + H^-$ for collisions.

$$H^+ + H^- \rightarrow H^+ + H^0(1s + 2s) + e^-$$
$$He^{+2} + H^- \rightarrow He^{+2} + H^0(1s + 2s) + e^-$$
$$Li^{+3} + H^- \rightarrow Li^{+3} + H^0(1s + 2s) + e^-$$

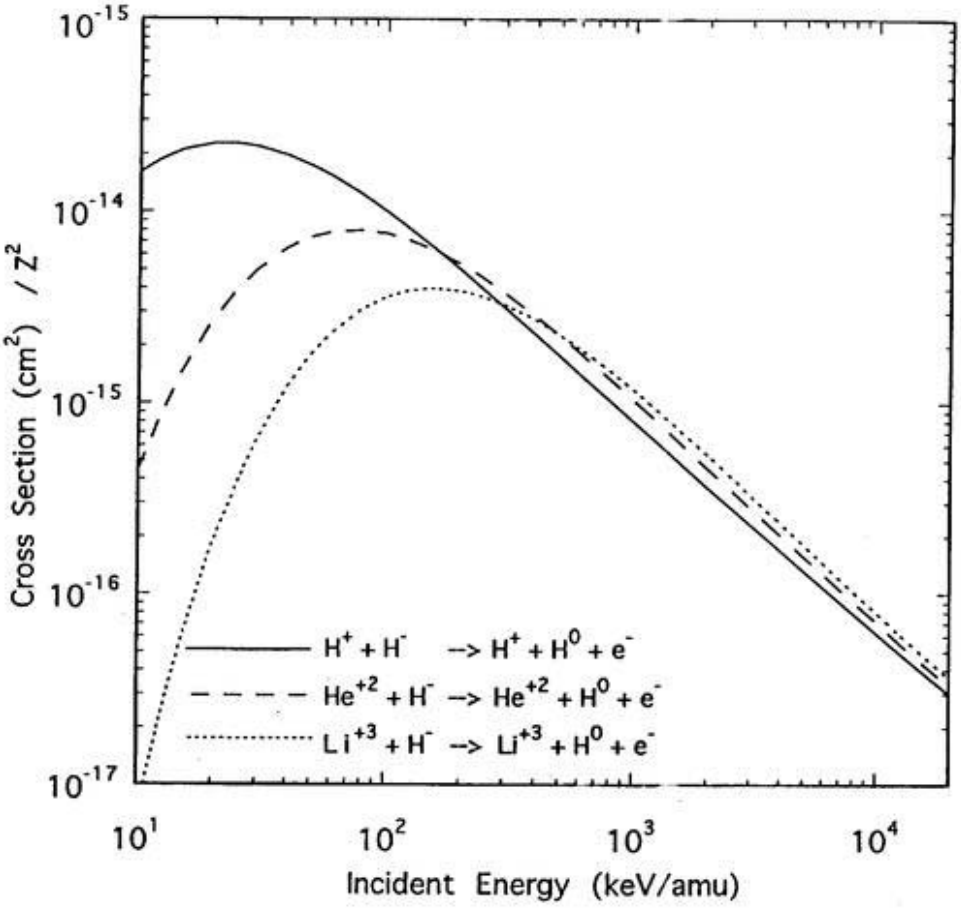

Figure 4.7: Comparison of the scaled cross sections (σ/Z^2) for electron detachment from H^- ions colliding with various positive ions. The solid line represents those for proton impact, the dashed line those for He^{+2} and the dotted line those for Li^{+3} ion impact. Note that the electron detachment cross sections are proportional to the square of positive ion charge at high energies.

References

Belkić Dž, 1977 J. Phys. B **10**, 3491

Belkić Dž, 1978 J. Phys. B **11**, 3529

Belkić Dž, 1997a Nucl. Instrum. Method. B **124**, 365

Belkić Dž, 1997b J. Phys. B **30**, 1731

Belkić Dž and Janev R K, 1973 J. Phys. B **6**, 1020

Belkić Dž and Mančev I, 1992 Phys. Scr. **45**, 35

Belkić Dž and Mančev I, 1993 Phys. Scr. **46**, 18

Belkić Dž, Mančev I and Mergel V, 1997 Phys. Rev. A **55**, 378

Cheshire I M, 1964 Proc. Phys. Soc. **84**, 89

Crothers D C F and McCann J F, 1983 J. Phys. B **16**, 2835

Dodd L D and Greider K R, 1966 Phys. Rev. **146**, 657

Fainstein P D, Ponce V H and Rivarola R D, 1990 J. Phys. B **23**, 1481

Fainstein P D, Ponce V H and Rivarola R D, 1991 J. Phys. B **24**, 3091

Gayet R, 1972 J. Phys. B **5**, 483

Gayet R, Hanssen J, Jacqui L, Martinez A and Rivarola R, 1996 Phys. Scr. **53**, 549

McDowell M R C and Coleman J P, 1970 *Introduction to the Theory of Ion-Atom Collisions*, (North-Holland Publishing Company)

Peart B, Walton D S and Dolder K T, 1970 J. Phys. B **3**, 1346

Peart B, Grey R and Dolder K T, 1976 J. Phys. B **23**, 3047

Shull H and Löwdin P -O, 1956 J. Chem. Phys. **25**, 1035

Tawara H, Tonuma T, Kumagai H, Imai T, Uskov D B and Presnyakov L P, 1999 Phys. Scr. (in printing)

5 Applications to NBI heating

5.1 Influence of present calculated results to NBI

The present studies of single electron detachment from H^- ions described above is useful for many applications, for example, plasma heating through Neutral atom Beam Injection (NBI) (Tawara 1995).

In fusion devices, it is necessary to heat the plasmas up to a few tens of keV in order to achieve nuclear fusion reactions. As most of fusion plasmas are confined by strong magnetic field, it is difficult to inject any charge particles into the devices. One of the most promising methods for plasma heating is the NBI. In order to obtain the high energy ($\sim$ MeV), powerful ($\sim$ MW) neutral hydrogen atom beam for NBI it is already known that H^- ions are converted into neutral hydrogen atoms, H^0, with better efficiencies as mentioned in Introduction. To diagnose the plasma density and temperature conditions in the main plasma, NBI is also used.

The knowledge of the cross sections of single electron detachment from H^- ions are indispensable to analyze the details relevant to NBI technique. Indeed, these data are very important in determining rates of conversion into neutral hydrogen (Janev *et al.* 1985, Shevelko and Vainshtein 1993, Tawara 1995 and Tawara and Russek 1973). The present calculated cross sections for production of the excited state hydrogen atoms are found to be relatively large compared with total cross sections, which had not been discussed in any past studies, and may influence the over-all conversion efficiencies.

By taken into account the contribution of H^0 atoms in the excited state, in particular of $H^0(2s)$ atoms, we consider the variation of fractions of H^- ions, H^0 atoms, $H^0(2s)$ atoms and H^+ ions when H^- ions are sent to neutralizing media

(such as neutral gas or plasma). It is assumed that $H^0(2p)$ atoms promptly decay into $H^0(1s)$ atoms. The rate equations for the fractions of these particles are given as follows (Tawara and Russek 1971):

$$\frac{dF_-}{dn} = -(\sigma_{-10(1s)} + \sigma_{-10(2s)})F_- \tag{5.1}$$

$$\frac{dF_{0(1s)}}{dn} = (\sigma_{-10(1s)}F_- - \sigma_{0(1s)1}F_0) \tag{5.2}$$

$$\frac{dF_{0(2s)}}{dn} = (\sigma_{-10(2s)}F_- - \sigma_{0(2s)1}F_{0(2s)}) \tag{5.3}$$

$$\frac{dF_+}{dn} = \sigma_{0(1s)1}F_0 + \sigma_{0(2s)1}F_{0(2s)} \tag{5.4}$$

$$F_- + F_{0(1s)} + F_{0(2s)} + F_+ = 1, \tag{5.5}$$

where n is the density of target particles and F_+, $F_{0(1s)}$, $F_{0(2s)}$ and F_- denote the fractions of H^+ ions, $H^0(1s)$ atoms in the ground state, $H^0(2s)$ atoms in the excited state and H^- ions, respectively. $\sigma_{-10(1s)}$, $\sigma_{-10(2s)}$, $\sigma_{0(1s)1}$ and $\sigma_{0(2s)1}$ denote the cross sections for H^- ion into $H^0(1s)$ atom, H^- ion into $H^0(2s)$ atom, $H^0(1s)$ atom into H^+ ion and $H^0(2s)$ atom into H^+ ion, respectively. Here we do not take into account the cross sections of excitation process for $H^0(1s)$ atom into $H^0(2s)$ atom which are assumed to be small at the present energy. We also neglect the double electron detachment processes from H^- ions into H^+ ions as the cross sections are expected to be two orders of magnitude smaller than those for single electron detachment (Tawara and Russek 1973).

We have already shown our calculated cross sections for H and H^+ impact (see Appendixes D.2 and D.3). The data of electron impact ionization cross sections for the excited $H^0(2s)$ atoms with the equivalent velocity of ion,

$$e^- + H^0(2s) \rightarrow e^- + H^+ + e^-, \tag{5.6}$$

and the data of proton impact cross sections for detachment process of H^0 atoms,

$$H^+ + H^0 \rightarrow H^+ + H^+ + e^-, \tag{5.7}$$

are taken from the experimental data (Defrance *et al.* 1981, Dxion *et al.* 1975, Fite *et al.* 1958).

In Fig. 5.1, we show the variation of fractions of H^- ions, $H^0(1s)$ atoms, $H^0(2s)$ atoms and H^+ ions in collisions with H atoms at 500 keV/amu incident energy. In Table 5.1 are shown the cross sections relevant to the present calculations. This figure indicates that, as the target density increases, the primary H^- ions decrease, meanwhile H^0 atoms increase. At the optimal target density, the H^0 atom fraction becomes maximum and, then, when the target density increase further, its fraction decreases due to the conversion of H^0 atoms into H^+ ions which finally become dominant over H^- ions and H^0 atoms. The highest conversion efficiencies into $H^0(1s)$ are found to be about 38 %, meanwhile those of $H^0(2s)$ atoms about 5 %. It is important to note that when the effects of the excited $H^0(2s)$ atom formation are excluded, they increase up to 42 %.

In a previous literature (Berkner *et al.* 1970) it has been shown that the neutralization efficiencies are 60 % of $D^-(H^-) + H_2$ collisions at the same collision energy. This difference of the conversion efficiencies is attributed to the magnitude of the cross sections in different targets, namely H and H_2. The observed cross section of $D^-(H^-) + H_2$ is larger than our calculated results.

On the other hand, in Fig. 5.2, we show the fractions of different particles in collisions with protons at 500 keV/amu incident energy. In Table 5.2 are shown the cross sections used in the rate equations. The highest conversion efficiencies into

$H^0(1s)$ are about 70 % and those into $H^0(2s)$ atoms below 1 %. Indeed, the plasma targets increase the conversion efficiencies for 500 keV/amu H^- ions, namely roughly by a factor of two. Another importance is the fact that the maximum conversion efficiencies can be obtained at the target densities which are roughly one order of magnitude smaller in H^+ ion target, compared with in those in H target atom. Practically $H^0(2s)$ state atom formation does not change the conversion efficiencies, as it is small, compared with H^0 state formation. We have shown that interactions with positive ions is provide much better conversion of H^- ions into neutral hydrogen atoms compared with neutral gases.

$\sigma_{-10(1s)}$	$\sigma_{-10(2s)}$	$\sigma_{0(1s)1}$	$\sigma_{0(2s)1}$
5.8×10^{-17}	3.7×10^{-18}	2.0×10^{-18}	3.9×10^{-17}

Table 5.1: The cross sections for H^- ions in collisions with H atoms used in the rate equations (5.1) $\sim$ (5.5)

$\sigma_{-10(1s)}$	$\sigma_{-10(2s)}$	$\sigma_{0(1s)1}$	$\sigma_{0(2s)1}$
1.8×10^{-15}	1.9×10^{-18}	2.2×10^{-17}	9.0×10^{-17}

Table 5.2: The cross sections for H^- ions in collisions with protons used in the rate equations (5.1) $\sim$ (5.5)

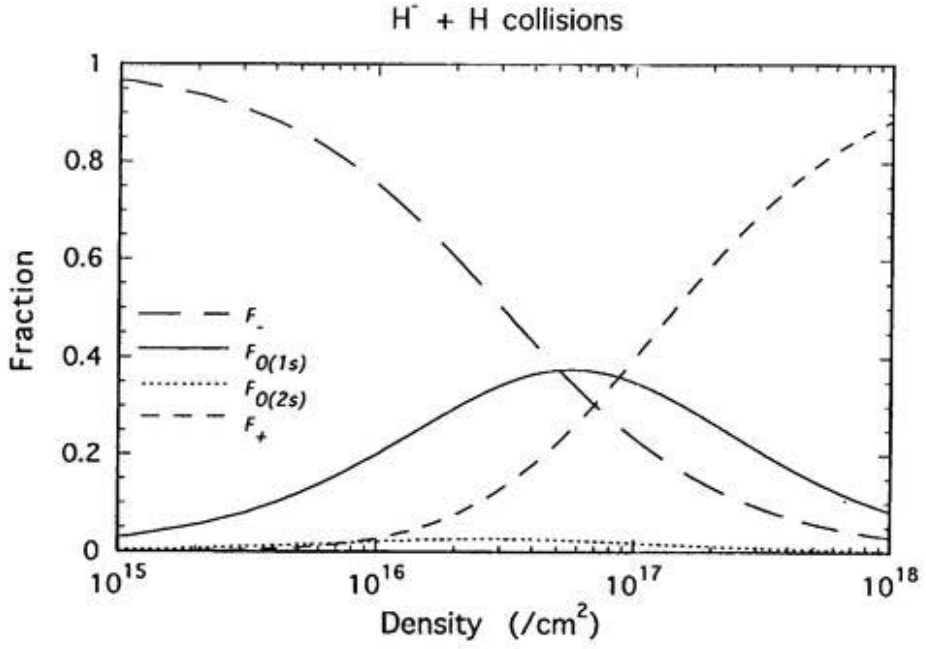

Figure 5.1: The fractions of H^- ions, $H^0(1s)$ atoms, $H^0(2s)$ atoms and H^+ ions in collisions with H atoms at 500 keV/amu as a function of target density. The long-dashed-curve represents the fraction of H^- ions, the solid-curve the fraction of $H^0(1s)$ atoms, the dotted-curve the fraction of $H^0(2s)$ and the short-dashed-curve the fraction of H^+ ions.

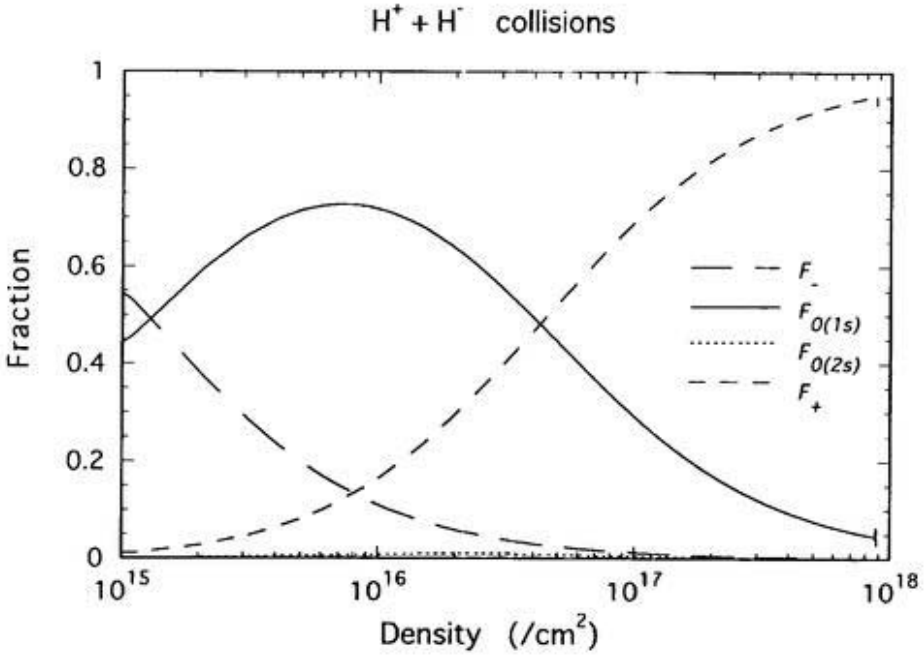

Figure 5.2: The fractions of H^- ions, $H^0(1s)$ atoms, $H^0(2s)$ atoms and H^+ ions in collisions with H^+ ions at 500 keV/amu as a function of target density. The long-dashed-curve represents the fraction of H^- ions, the solid-curve the fraction of $H^0(1s)$ atoms, the dotted-curve the fraction of $H^0(2s)$ and the short-dashed-curve the fraction of H^+ ions.

References

Berkner K H, Pyle R V and Stearns J W, 1975 Nucl. Fus. **15**, 249

Defrance P, Claeys W, Cornet A and Poulaert Q, 1981 J. Phys. B **14**, 111

Dixion A J, von Engel A and Harrison M F A, 1975 Proc. R. Soc. London A **343**, 333

Fite W L and Brackmann R T, 1958 Phys. Rev. **112**, 1141

Janev R K, Presnyakov L P and Shevelko V P, 1985 *Physics of Highly Charged Ions*, Springer-Verlag, Berlin, Heidelberg, New York, Tokyo

Shevelko V P and Vainstein L A, 1993 *Atomic Physics for Hot Plasmas*, Institute of Physics Publishing, Bristol and Philadelphia

Tawara H, 1995 Heavy Ion Phys. **1**, 133

Tawara H and Russek A, 1973 Rev. Mod. Phys. **45**, 178

6 Future problems

6.1 Double electron detachment

In this section, we discuss some of future problems in the analysis of electron detachment processes.

In this thesis, we have treated only the single electron detachment processes of H^- ions. However, the double electron detachment from H^- ion processes is an interesting topics. We briefly consider some effects for double electron detachment here.

Firstly, we consider the correlation of two free electrons in the exit channel. Here we introduce the following formula:

$$\Phi_f = \phi_{e^-_{Z(j)},e^-_{Z(j')}}(\boldsymbol{x}_1,\boldsymbol{x}_2)g(\boldsymbol{r}_{12}), \tag{6.1}$$

$$\boldsymbol{r}_{12} = \boldsymbol{r}_1 - \boldsymbol{r}_2 \tag{6.2}$$

where $\phi_{e^-_{Z(j)},e^-_{Z(j')}}$ indicates the two detached electron wave function. This form is given as follows:

$$\begin{aligned}&\phi_{e^-_{Z(j)},e^-_{Z(j')}}(\boldsymbol{x}_1,\boldsymbol{x}_2)\\ =\ &\frac{1}{\sqrt{2}}\{\phi_{e^-_{Z(j)}}(\boldsymbol{x}_1,\boldsymbol{k}_1)\phi_{e^-_{Z(j')}}(\boldsymbol{x}_2,\boldsymbol{k}_2)+\phi_{e^-_{Z(j)}}(\boldsymbol{x}_2,\boldsymbol{k}_1)\phi_{e^-_{Z(j')}}(\boldsymbol{x}_1,\boldsymbol{k}_2)\},\end{aligned} \tag{6.3}$$

$$\tag{6.4}$$

where $\phi_{e^-_{Z(j)}}$ and $\phi_{e^-_{Z(j')}}$ indicate the electron detachment wave functions which are given as follows:

$$\phi_{e^-_Z}(\boldsymbol{x}_i) = N(\zeta_Z)\,{}_1F_1\Big(i\zeta_Z,1,i\{\kappa x_i-\boldsymbol{\kappa}\cdot\boldsymbol{x}_i\}\Big)e^{i\boldsymbol{\kappa}\cdot\boldsymbol{x}_i} \tag{6.5}$$

$$N(\zeta_Z) = \frac{\Gamma(1-\zeta_Z)e^{\pi\zeta_Z}}{(2\pi)^{3/2}}$$

$$\boldsymbol{\kappa} = \boldsymbol{k}_1 \text{ or } \boldsymbol{k}_2$$

$$Z = Z(j) \text{ or } Z(j'),$$

where $Z(j)$ and $Z(j')$ represent the effective charge of each electron in H^- ion, namely $Z(1s)$ or $Z(1s')$ (see Eqs. (2.4) and (2.5)) and $g(\boldsymbol{r}_{12})$ the correlation effect. Pluvinage (1951) and Munschy and Pluvinage (1954) introduced the same function of the correlation effect for helium atom which depend on the scaler r_{12}. However, we have to introduce $g(\boldsymbol{r}_{12})$ in Eq. (6.1) which includes the vector $\boldsymbol{r}_{12}$ because two free electrons have their momenta, $\boldsymbol{k}_1$ and $\boldsymbol{k}_2$, and each electron is separated out in the following momentum:

$$\boldsymbol{k} = \boldsymbol{k}_1 - \boldsymbol{k}_2. \tag{6.6}$$

And $g(\boldsymbol{r}_{12})$ satisfies the following differential equation,

$$(-\frac{1}{2}\nabla^2_{\boldsymbol{r}_{12}} + \frac{1}{r_{12}} - k^2)g(\boldsymbol{r}_{12}) = 0. \tag{6.7}$$

Then the solution of Eq. (6.7) is given as follows:

$$g(\boldsymbol{r}_{12}) = e^{\pi\nu}\Gamma(1+i\nu)_1F_1(-i\nu, 1, -ikr_{12} - i\boldsymbol{k}\cdot\boldsymbol{r}_{12}), \tag{6.8}$$

$$\nu = \frac{1}{k}.$$

Equation (6.8) represents the correlation effect for the two free electrons.

In the present work, we have not treated this effect. However the correlation effect between two out-going free electrons is important in the two electron detachment processes from H^- ions.

References

Pluvinage P, 1951 J. Phys. Radium **12**, 78

Munschy G and Pluvinage P, 1954 J. Phys. Radium **15**, 122

7 Conclusion

We have presented the calculated single electron detachment cross sections from H^- ions in collisions with neutral atoms and bare positive ions at high energies.

In the present theoretical analysis, we have treated independently two electrons in H^- ions, the loosely bound 1s' electron and the tightly bound 1s electron. The calculated results show that the dominant contribution to electron detachment comes from the loosely bound 1s' electron in the production of the ground state hydrogen atoms, $H^0(1s)$. On the other hand, in the production of the excited state hydrogen atoms, $H^0(2s)$ and H(2p), the tightly bound 1s electron detachment is dominant over the loosely bound 1s' electron detachment. it has also been found that our calculated results for total and also partial cross sections for helium target are in good agreement with experimental data at high energies (> 100 keV) but are in some discrepancies at low energy range. The discrepancy is due to the first Born approximation which we have used throughout the present calculations. In particular, it should be noted from the present detailed calculations that atomic hydrogens in the excited states formed in electron detachment processes can significantly change the overall conversion efficiencies of H^- ions into neutral hydrogen atoms in applications to NBI and to plasma diagnostics.

In collisions with various positive ions, we have calculated the single electron detachment cross sections of H^- ions based on the 4-B CDW-EIS approximation. The present calculated results clearly show that the electron detachment cross sections in collisions with protons, though still no experimental data are available to compare, are one order of magnitude larger than those with neutral hydrogen atoms. It has also been found that the cross sections of single electron detachment from H^- ions

in collisions with various bare positive ions are proportional to the square of positive ion charge, at least, in high energy region.

In collisions with neutral atoms and positive ions, though the cross sections of the single electron detachment from H^- ions are different size, we note similar features in formation of the excited states of H^0 atoms, the electron detachment process of the tightly bound electron (1s) is dominant over the loosely bound 1s' the electron detachment process. This is understood due to the fact that, in the processes of production of the excited states, $H^0(2s)$ and $H^0(2p)$ atoms, their energy levels are close to the 1s' electron energy level in H^- ion.

Finally, we would like to point out two important consequences obtained in the present work from the view point of applications to NBI, compared with those in collisions with neutral atoms which are presently in use:

i) Higher conversion efficiencies from H^- ions to H^0 atoms in collisions with positive ions,

ii) Lower target densities for getting optimum conversion efficiencies in collision with positive ions

Thus, the present results suggest that the plasma targets are quite promising in converting H^- ions into H^0 atoms in use of powerful NBI for effective plasma heating.

Appendix

A The wave function for the detached electron

The total electronic Hamiltonian of hydrogen atom and a detached electron system is given as

$$H = -\frac{\nabla^2_{\boldsymbol{x}_1}}{2} - \frac{\nabla^2_{\boldsymbol{x}_2}}{2} - \frac{1}{x_1} - \frac{1}{x_2} + \frac{1}{x_{12}}. \tag{A.1}$$

And the wave function in the exit channel Ψ_f is given as follows:

$$\Psi_f = \Phi_{H^0(nlm)}(\boldsymbol{x}_1)\Phi_{e^-_{Z(j)}}(\boldsymbol{x}_2). \tag{A.2}$$

Equations (A.1) and (A.2) satisfy the following Schrödinger equation:

$$(-\frac{\nabla^2_{\boldsymbol{x}_1}}{2} - \frac{\nabla^2_{\boldsymbol{x}_2}}{2} - \frac{1}{x_1} - \frac{1}{x_2} + \frac{1}{x_{12}} - E_f)\Phi_{H^0(nlm)}(\boldsymbol{x}_1)\Phi_{e^-_{Z(j)}}(\boldsymbol{x}_2) = 0, \tag{A.3}$$

$$E_f = E_{H^0(nlm)} + E_\kappa$$

$$E_\kappa = \frac{\kappa^2}{2} \tag{A.4}$$

where $E_{H^0(nlm)}$ is the binding energy of H^0(nlm) atom, E_κ the kinetic energy of the detached electron, κ the wave number of the detached electron. The wave function of hydrogen atom In Eq. (A.3) satisfy the following differential equation:

$$(-\frac{\nabla^2_{\boldsymbol{x}_1}}{2} - \frac{1}{x_1} - E_{H^0})\Phi_{H^0(nlm)}(\boldsymbol{x}_1) = 0. \tag{A.5}$$

The remaining differential equation form of Eq. (A.3) is

$$(-\frac{\nabla^2_{\boldsymbol{x}_2}}{2} - \frac{1}{x_2} + \frac{1}{x_{12}} - E_\kappa)\Phi_{e^-_{Z(j)}}(\boldsymbol{x}_2) = 0. \tag{A.6}$$

Immediately after collisions, the second and third terms in Eq. (A.6) are approximately given as follows:

$$-\frac{1}{x_2} + \frac{1}{x_{12}} \simeq -\frac{Z(j)^2}{x_2}, \tag{A.7}$$

where $Z(j)$ is the effective nuclear charge felt by each electron in H^- ion. Then, Eq. (A.6) can be rewritten as

$$(-\frac{\nabla^2_{\boldsymbol{x}_2}}{2} - \frac{Z(j)^2}{x_2} - \frac{\kappa^2}{2})\Phi_{e^-_{Z(j)}}(\boldsymbol{x}_2) = 0. \tag{A.8}$$

The wave function for the detached electron form

$$\begin{aligned} \Phi_{e^-_{Z(j)}}(\boldsymbol{x}_2) &= N(\zeta_{Z(j)})_1F_1\Big(i\zeta_{Z(j)}, 1, i\{\kappa x_2 - \boldsymbol{\kappa}\cdot\boldsymbol{x}_2\}\Big)e^{i\boldsymbol{\kappa}\cdot\boldsymbol{x}_2} \qquad (A.9) \\ N(\zeta_{Z(j)}) &= \frac{\Gamma(1-\zeta_{Z(j)})e^{\pi\zeta_{Z(j)}}}{(2\pi)^{3/2}}. \end{aligned}$$

satisfies Eq. (A.8) (Abramowitz and Stegun 1970)

Reference

Abramowitz M and Stegun I A, 1970 *Handbook of Mathematical Functions*, Dover Publications Inc. New York

B Distorted potential in the entrance channel

We choose the distorted wave function in the entrance channel as follows:

$$\Psi^+ = \Phi_{H^-}(\boldsymbol{x}_1, \boldsymbol{x}_2)e^{-iE_at}e^{-i\nu_{a'}ln(vs_1+\boldsymbol{v}\cdot\boldsymbol{s}_1)}e^{-i\nu_{a''}ln(vR-\boldsymbol{v}\cdot\boldsymbol{R})}, \tag{B.1}$$

and this wave function satisfies Eq. (4.23):

$$(H_i - i\frac{\partial}{\partial t})\Psi^+ = V_{d_a}\Psi^+. \tag{B.2}$$

The L.H.S. of Eq. (B.2) can be rewritten as:

$$
\begin{aligned}
& (H_i - i\frac{\partial}{\partial t})\Psi^+ \\
= \; & (-\frac{1}{2}\nabla^2_{\boldsymbol{x}_1} - \frac{1}{2}\nabla^2_{\boldsymbol{x}_2} \\
& -\frac{1}{x_1} - \frac{1}{x_2} + \frac{1}{r_{12}} - i\frac{\partial}{\partial t})\Phi_{H^-}(\boldsymbol{x}_1, \boldsymbol{x}_2) e^{-iE_a t} e^{-i\nu_{a'} ln(vs_1 + \boldsymbol{v}\cdot\boldsymbol{s}_1)} e^{-i\nu_{a''} ln(vR - \boldsymbol{v}\cdot\boldsymbol{R})} \\
& +\Phi_{H^-}(\boldsymbol{x}_1, \boldsymbol{x}_2) e^{-iE_a t} \frac{1}{2}\nabla^2_{\boldsymbol{x}_1} e^{-i\nu_{a'} ln(vs_1 + \boldsymbol{v}\cdot\boldsymbol{s}_1)} e^{-i\nu_{a''} ln(vR - \boldsymbol{v}\cdot\boldsymbol{R})} \\
& -\nabla_{\boldsymbol{x}_1}\Phi_{H^-}(\boldsymbol{x}_1, \boldsymbol{x}_2) e^{-iE_a t} \frac{1}{2}\nabla_{\boldsymbol{s}_1} e^{-i\nu_{a'} ln(vs_1 + \boldsymbol{v}\cdot\boldsymbol{s}_1)} e^{-i\nu_{a''} ln(vR - \boldsymbol{v}\cdot\boldsymbol{R})} \\
& +(\frac{Z}{R} - \frac{Z}{s_1} - \frac{Z}{s_2})\Phi_{H^-}(\boldsymbol{x}_1, \boldsymbol{x}_2) e^{-iE_a t} e^{-i\nu_{a'} ln(vs_1 + \boldsymbol{v}\cdot\boldsymbol{s}_1)} e^{-i\nu_{a''} ln(vR - \boldsymbol{v}\cdot\boldsymbol{R})} \\
& -i\Phi_{H^-}(\boldsymbol{x}_1, \boldsymbol{x}_2) e^{-iE_a t} \frac{\partial}{\partial t} e^{-i\nu_{a'} ln(vs_1 + \boldsymbol{v}\cdot\boldsymbol{s}_1)} e^{-i\nu_{a''} ln(vR - \boldsymbol{v}\cdot\boldsymbol{R})}. \qquad \text{(B.3)}
\end{aligned}
$$

Equation (B.3) can be rewritten as follows:

$$
\begin{aligned}
& (-\frac{Z}{v}\frac{1}{v}(vs_1 + \boldsymbol{v}\cdot\boldsymbol{s}_1)^{-i\nu_{a'}-1} e^{-i\nu_{a''} ln(vR - \boldsymbol{v}\cdot\boldsymbol{R})} \\
& -\nabla_{\boldsymbol{x}_1}\Phi_{H^-}(\boldsymbol{x}_1, \boldsymbol{x}_2) e^{-iE_a t} \frac{1}{2}\nabla_{\boldsymbol{s}_1} e^{-i\nu_{a'} ln(vs_1 + \boldsymbol{v}\cdot\boldsymbol{s}_1)} e^{-i\nu_{a''} ln(vR - \boldsymbol{v}\cdot\boldsymbol{R})} \\
& +(\frac{Z}{R} - \frac{Z}{s_1} - \frac{Z}{s_2})\Phi_{H^-}(\boldsymbol{x}_1, \boldsymbol{x}_2) e^{-iE_a t} e^{-i\nu_{a'} ln(vs_1 + \boldsymbol{v}\cdot\boldsymbol{s}_1)} e^{-i\nu_{a''} ln(vR - \boldsymbol{v}\cdot\boldsymbol{R})} \\
& -(\frac{Z(Z_{H^-} - 1)}{R} - \frac{Z}{s_1})\Phi_{H^-}(\boldsymbol{x}_1, \boldsymbol{x}_2) e^{-iE_a t} e^{-i\nu_{a'} ln(vs_1 + \boldsymbol{v}\cdot\boldsymbol{s}_1)} e^{-i\nu_{a''} ln(vR - \boldsymbol{v}\cdot\boldsymbol{R})} \qquad \text{(B.4)} \\
= \; & V_{d_a}\Psi^+.
\end{aligned}
$$

The final form of the distorted potential V_{d_a} is

$$
\begin{aligned}
V_{d_a}\Psi^+ \; = \; & (-\frac{Z}{v}\frac{1}{v}(vs_1 + \boldsymbol{v}\cdot\boldsymbol{s}_1)^{-i\nu_{a'}-1} e^{-i\nu_{a''} ln(vR - \boldsymbol{v}\cdot\boldsymbol{R})} \\
& -\nabla_{\boldsymbol{x}_1}\Phi_{H^-}(\boldsymbol{x}_1, \boldsymbol{x}_2) e^{-iE_a t} \frac{1}{2}\nabla_{\boldsymbol{s}_1} e^{-i\nu_{a'} ln(vs_1 + \boldsymbol{v}\cdot\boldsymbol{s}_1)} e^{-i\nu_{a''} ln(vR - \boldsymbol{v}\cdot\boldsymbol{R})} \\
& +(\frac{Z}{R} - \frac{Z}{s_2})\Phi_{H^-}(\boldsymbol{x}_1, \boldsymbol{x}_2) e^{-iE_a t} e^{-i\nu_{a'} ln(vs_1 + \boldsymbol{v}\cdot\boldsymbol{s}_1)} e^{-i\nu_{a''} ln(vR - \boldsymbol{v}\cdot\boldsymbol{R})}.
\end{aligned}
$$

C Distorted potential in the exit channel

We choose the distorted wave function in the exit channel as follows:

$$\Psi^- = \phi_b(\boldsymbol{x}_1, \boldsymbol{x}_2)$$

$$\times e^{\pi\nu_{b'}}\Gamma(1+i\nu_{b'})_1F_1(-i\nu_{b'}, 1, -ips_1 - i\boldsymbol{p}\cdot\boldsymbol{s}_1)e^{-i\nu_{b''}ln(vR+\boldsymbol{v}\cdot\boldsymbol{R})} \quad (C.1)$$

$$\nu_{b'} = \frac{Z}{p}, \quad \nu_{b''} = \frac{Z(Z_{H^-}-1)}{v}. \quad (C.2)$$

and this wave function satisfies Eq. (4.34):

$$(H_f - i\frac{\partial}{\partial t})\Psi^- = V_{d_b}\Psi^+. \quad (C.3)$$

The L.H.S. of Eq. (C.3) can be rewritten as:

$$(H_f - i\frac{\partial}{\partial t})\Psi^-$$

$$= \phi_b(\boldsymbol{x}_1, \boldsymbol{x}_2)(-\frac{1}{2}\nabla^2_{\boldsymbol{x}_1})\Gamma(1+i\nu_{b'})_1F_1(-i\nu_{b'}, 1, -ips_1 - i\boldsymbol{p}\cdot\boldsymbol{s}_1)e^{-i\nu_{b''}ln(vR+\boldsymbol{v}\cdot\boldsymbol{R})}$$

$$+(-\frac{1}{s_1} - \frac{1}{s_2} - \frac{1}{x_1} + \frac{1}{r_{12}} + \frac{1}{R})$$

$$\times\phi_b(\boldsymbol{x}_1, \boldsymbol{x}_2)e^{\pi\nu_{b'}}\Gamma(1+i\nu_{b'})_1F_1(-i\nu_{b'}, 1, -ips_1 - i\boldsymbol{p}\cdot\boldsymbol{s}_1)e^{-i\nu_{b''}ln(vR+\boldsymbol{v}\cdot\boldsymbol{R})}$$

$$-\phi_b(\boldsymbol{x}_1, \boldsymbol{x}_2)i\frac{\partial}{\partial t}e^{\pi\nu_{b'}}\Gamma(1+i\nu_{b'})_1F_1(-i\nu_{b'}, 1, -ips_1 - i\boldsymbol{p}\cdot\boldsymbol{s}_1)e^{-i\nu_{b''}ln(vR+\boldsymbol{v}\cdot\boldsymbol{R})}$$

$$= V_{d_b}\Psi^+ \quad (C.4)$$

and the wave function (C.1) satisfies the following differential equation:

$$(\frac{1}{2}\nabla^2_{\boldsymbol{s}_1} - \frac{1}{s_1} - i\boldsymbol{\kappa}\cdot\nabla_{\boldsymbol{s}_1} - i\frac{\partial}{\partial t})$$

$$\times e^{\pi\nu_{b'}}\Gamma(1+i\nu_{b'})_1F_1(-i\nu_{b'}, 1, -ips_1 - i\boldsymbol{p}\cdot\boldsymbol{s}_1)e^{-i\nu_{b''}ln(vR+\boldsymbol{v}\cdot\boldsymbol{R})} = 0, \quad (C.5)$$

where

$$\nabla_{\boldsymbol{s}_1} = \nabla_{\boldsymbol{x}_1}. \quad (C.6)$$

Using Eqs. (C.4) and (C.5), the final form of the distorted potential is as follows:

$$V_{d_b} = (\frac{Z}{R} - \frac{Z}{s_2}) + (\frac{1}{r_{12}} - \frac{1}{x_1}). \tag{C.7}$$

D Numerical tables for electron detachment cross sections from H^- ions

We summarize our calculated cross sections in the following tables where the cross sections in units of cm^2 are given against the laboratory incident energy in units of keV/amu.

D.1 Collisions with helium atoms

$$H^- + He \rightarrow H^0(1s,\ 2s \text{ and } 2p) + e^- + \sum_{n'} He(n')$$

$E(keV/amu)$	$\sigma_{H^0(1s)}$	$\sigma_{H^0(2s)}$	$\sigma_{H^0(2p)}$	σ_{sum}
10	8.5724×10^{-16}	9.4413×10^{-17}	1.2147×10^{-17}	9.6380×10^{-16}
20	5.6374×10^{-16}	8.5389×10^{-17}	1.9615×10^{-17}	6.6875×10^{-16}
30	4.3352×10^{-16}	7.1122×10^{-17}	2.9686×10^{-17}	5.3433×10^{-16}
40	3.5754×10^{-16}	5.9201×10^{-17}	2.9824×10^{-17}	4.4657×10^{-16}
50	3.0756×10^{-16}	5.0804×10^{-17}	2.7603×10^{-17}	3.8597×10^{-16}
60	2.7141×10^{-16}	4.4729×10^{-17}	2.5157×10^{-17}	3.4130×10^{-16}
80	2.2201×10^{-16}	3.6483×10^{-17}	2.1032×10^{-17}	2.7953×10^{-16}
100	1.8944×10^{-16}	3.1082×10^{-17}	1.7983×10^{-17}	2.3850×10^{-16}
200	1.1378×10^{-16}	1.8518×10^{-17}	1.0455×10^{-17}	1.4276×10^{-16}
300	8.3210×10^{-17}	1.3533×10^{-17}	7.4235×10^{-18}	1.0417×10^{-16}
400	6.6514×10^{-17}	1.0803×10^{-17}	5.7749×10^{-18}	8.3091×10^{-17}
500	5.5608×10^{-17}	9.0602×10^{-18}	4.7339×10^{-18}	6.9402×10^{-17}
600	4.7905×10^{-17}	7.8303×10^{-18}	4.0150×10^{-18}	5.9750×10^{-17}
800	3.6510×10^{-17}	6.1724×10^{-18}	3.0843×10^{-18}	4.5767×10^{-17}
1000	2.9361×10^{-17}	5.1114×10^{-18}	2.5067×10^{-18}	3.6979×10^{-17}
2000	1.4870×10^{-17}	2.8352×10^{-18}	1.2994×10^{-18}	1.9004×10^{-17}
3000	9.9983×10^{-18}	2.0010×10^{-18}	8.7849×10^{-19}	1.2878×10^{-17}
4000	7.5423×10^{-18}	1.5577×10^{-18}	6.6391×10^{-19}	9.7639×10^{-18}
5000	6.0506×10^{-18}	1.2807×10^{-18}	5.3369×10^{-19}	7.8649×10^{-18}
6000	5.0475×10^{-18}	1.0893×10^{-18}	4.4623×10^{-19}	6.5831×10^{-18}
8000	3.7988×10^{-18}	8.4141×10^{-19}	3.3613×10^{-19}	4.9763×10^{-18}
10000	3.0479×10^{-18}	6.8712×10^{-19}	2.6963×10^{-19}	4.0046×10^{-18}

D.2 Collisions with hydrogen atoms

$$H^- + H \rightarrow H^0(1s,\ 2s \text{ and } 2p) + e^- + \sum_{n'} H(n')$$

$E(keV/amu)$	$\sigma_{H^0(1s)}$	$\sigma_{H^0(2s)}$	$\sigma_{H^0(2p)}$	σ_{sum}
10	7.9258×10^{-16}	6.3712×10^{-17}	2.1974×10^{-18}	8.5849×10^{-16}
20	5.6096×10^{-16}	5.4849×10^{-17}	5.7760×10^{-18}	6.2159×10^{-16}
30	4.4243×10^{-16}	4.2310×10^{-17}	7.0487×10^{-18}	4.9179×10^{-16}
40	3.6919×10^{-16}	3.4471×10^{-17}	7.3749×10^{-18}	4.1103×10^{-16}
50	3.1877×10^{-16}	2.9456×10^{-17}	7.3812×10^{-18}	3.5560×10^{-16}
60	2.8162×10^{-16}	2.5991×10^{-17}	7.2549×10^{-18}	3.1487×10^{-16}
80	2.3007×10^{-16}	2.1437×10^{-17}	6.8591×10^{-18}	2.5837×10^{-16}
100	1.9565×10^{-16}	1.8495×10^{-17}	6.4238×10^{-18}	2.2057×10^{-16}
200	1.1536×10^{-16}	1.1627×10^{-18}	4.7143×10^{-18}	1.3170×10^{-16}
300	8.3490×10^{-17}	8.8180×10^{-18}	3.6970×10^{-18}	9.6005×10^{-17}
400	6.6035×10^{-17}	7.2379×10^{-18}	3.0421×10^{-18}	7.6315×10^{-17}
500	5.4912×10^{-17}	6.2042×10^{-18}	2.5864×10^{-18}	6.3703×10^{-17}
600	4.7135×10^{-17}	5.4607×10^{-18}	2.2509×10^{-18}	5.4847×10^{-17}
800	3.5949×10^{-17}	4.4286×10^{-18}	1.7894×10^{-18}	4.2167×10^{-17}
1000	2.8948×10^{-17}	3.7445×10^{-18}	1.4865×10^{-18}	3.4179×10^{-17}
2000	1.4727×10^{-17}	2.1998×10^{-18}	8.0852×10^{-19}	1.7736×10^{-17}
3000	9.8999×10^{-18}	1.5957×10^{-18}	5.5652×10^{-19}	1.2052×10^{-17}
4000	7.4625×10^{-18}	1.2635×10^{-18}	4.2461×10^{-19}	9.1506×10^{-18}
5000	5.9907×10^{-18}	1.0506×10^{-18}	3.4338×10^{-19}	7.3847×10^{-18}
6000	5.0051×10^{-18}	9.0149×10^{-19}	2.8830×10^{-19}	6.1949×10^{-18}
8000	3.7674×10^{-18}	7.0517×10^{-19}	2.1835×10^{-19}	4.6909×10^{-18}
10000	3.0212×10^{-18}	5.8088×10^{-19}	1.7576×10^{-19}	3.7778×10^{-18}

D.3 Collisions with protons

$H^+ + H^- \rightarrow H^+ + H^0(1s \text{ and } 2s) + e^-$

$E(keV/amu)$	$\sigma_{H^0(1s)}$	$\sigma_{H^0(2s)}$	σ_{sum}
10	1.5944×10^{-14}	5.2147×10^{-18}	1.5949×10^{-14}
20	2.2642×10^{-14}	1.1793×10^{-17}	2.2654×10^{-14}
30	2.1898×10^{-14}	1.4087×10^{-17}	2.1912×10^{-14}
40	1.9677×10^{-14}	1.4507×10^{-17}	1.9691×10^{-14}
50	1.7409×10^{-14}	1.4189×10^{-17}	1.7423×10^{-14}
60	1.5410×10^{-14}	1.3594×10^{-17}	1.5424×10^{-14}
80	1.2294×10^{-14}	1.2235×10^{-17}	1.2306×10^{-14}
100	1.0080×10^{-14}	1.0983×10^{-17}	1.0091×10^{-14}
200	4.9811×10^{-15}	7.0991×10^{-18}	4.9882×10^{-15}
300	3.1791×10^{-15}	5.2522×10^{-18}	3.1843×10^{-15}
400	2.2937×10^{-15}	4.1890×10^{-18}	2.2979×10^{-15}
500	1.7766×10^{-15}	3.4971×10^{-18}	1.7801×10^{-15}
600	1.4411×10^{-15}	3.0096×10^{-18}	1.4441×10^{-15}
800	1.0356×10^{-15}	2.3656×10^{-18}	1.0380×10^{-15}
1000	8.0211×10^{-16}	1.9572×10^{-18}	8.0406×10^{-16}
2000	3.6557×10^{-16}	1.0737×10^{-18}	3.6664×10^{-16}
3000	2.3251×10^{-16}	7.4960×10^{-19}	2.3326×10^{-16}
4000	1.6924×10^{-16}	5.7874×10^{-19}	1.6982×10^{-16}
5000	1.3252×10^{-16}	4.7252×10^{-19}	1.3299×10^{-16}
6000	1.0866×10^{-16}	3.9980×10^{-19}	1.0906×10^{-16}
8000	7.9593×10^{-17}	3.0631×10^{-19}	7.9899×10^{-17}
10000	6.2622×10^{-17}	2.4857×10^{-19}	6.2871×10^{-17}

D.4 Collisions with He^{+2} ions

$He^{+2} + H^- \rightarrow He^{+2} + H^0(1s \text{ and } 2s) + e^-$

$E(keV/amu)$	$\sigma_{H^0(1s)}$	$\sigma_{H^0(2s)}$	σ_{sum}
10	1.7811×10^{-15}	5.8230×10^{-19}	1.7817×10^{-15}
20	1.0805×10^{-14}	5.6199×10^{-18}	1.0811×10^{-14}
30	1.9800×10^{-14}	1.2707×10^{-17}	1.9813×10^{-14}
40	2.5919×10^{-14}	1.9046×10^{-17}	2.5938×10^{-14}
50	2.9511×10^{-14}	2.3957×10^{-17}	2.9535×10^{-14}
60	3.1346×10^{-14}	2.7526×10^{-17}	3.1374×10^{-14}
80	3.2006×10^{-14}	3.1682×10^{-17}	3.2038×10^{-14}
100	3.0774×10^{-14}	3.3334×10^{-17}	3.0807×10^{-14}
200	2.1330×10^{-14}	3.0201×10^{-17}	2.1361×10^{-14}
300	1.5162×10^{-14}	2.4892×10^{-17}	1.5187×10^{-14}
400	1.1454×10^{-14}	2.0796×10^{-17}	1.1475×10^{-14}
500	9.0679×10^{-15}	1.7753×10^{-17}	9.0857×10^{-15}
600	7.4341×10^{-15}	1.5448×10^{-17}	7.4495×10^{-15}
800	5.3763×10^{-15}	1.2227×10^{-17}	5.3885×10^{-15}
1000	4.1558×10^{-15}	1.0101×10^{-17}	4.1659×10^{-15}
2000	1.8401×10^{-15}	5.3913×10^{-18}	1.8455×10^{-15}
3000	1.1420×10^{-15}	3.6752×10^{-18}	1.1456×10^{-15}
4000	8.1618×10^{-16}	2.7872×10^{-18}	8.1897×10^{-16}
5000	6.3014×10^{-16}	2.2444×10^{-18}	6.3239×10^{-16}
6000	5.1095×10^{-16}	1.8781×10^{-18}	5.1283×10^{-16}
8000	3.6796×10^{-16}	1.4151×10^{-18}	3.6938×10^{-16}
10000	2.8594×10^{-16}	1.1343×10^{-18}	2.8707×10^{-16}

D.5 Collisions with Li^{+3} ions

$Li^{+3} + H^- \rightarrow Li^{+3} + H^0(1s \text{ and } 2s) + e^-$

$E(keV/amu)$	$\sigma_{H^0(1s)}$	$\sigma_{H^0(2s)}$	σ_{sum}
10	6.2964×10^{-17}	2.0585×10^{-20}	6.2985×10^{-17}
20	1.6349×10^{-15}	8.5034×10^{-19}	1.6358×10^{-15}
30	5.7053×10^{-15}	3.6611×10^{-18}	5.7089×10^{-15}
40	1.0963×10^{-14}	8.0553×10^{-18}	1.0972×10^{-14}
50	1.6220×10^{-14}	1.3164×10^{-17}	1.6233×10^{-14}
60	2.0898×10^{-14}	1.8345×10^{-17}	2.0916×10^{-14}
80	2.7960×10^{-14}	2.7662×10^{-17}	2.7988×10^{-14}
100	3.2294×10^{-14}	3.4953×10^{-17}	3.2329×10^{-14}
200	3.4826×10^{-14}	4.9225×10^{-17}	3.4875×10^{-14}
300	2.9621×10^{-14}	4.8526×10^{-17}	2.9670×10^{-14}
400	2.4638×10^{-14}	4.4626×10^{-17}	2.4683×10^{-14}
500	2.0685×10^{-14}	4.0396×10^{-17}	2.0726×10^{-14}
600	1.7627×10^{-14}	3.6536×10^{-17}	1.7663×10^{-14}
800	1.3347×10^{-14}	3.0280×10^{-17}	1.3377×10^{-14}
1000	1.0576×10^{-14}	2.5647×10^{-17}	1.0601×10^{-14}
2000	4.8369×10^{-15}	1.4147×10^{-17}	4.8510×10^{-15}
3000	2.9975×10^{-15}	9.6342×10^{-18}	3.0072×10^{-15}
4000	2.1293×10^{-15}	7.2637×10^{-18}	2.1366×10^{-15}
5000	1.6332×10^{-15}	5.8118×10^{-18}	1.6390×10^{-15}
6000	1.3162×10^{-15}	4.8341×10^{-18}	1.3210×10^{-15}
8000	9.3791×10^{-16}	3.6047×10^{-18}	9.4152×10^{-16}
10000	7.2268×10^{-16}	2.8655×10^{-18}	7.2555×10^{-16}

Acknowledgments

The present author wishes to thank Prof. Hiroyuki Tawara (National Institute for Fusion Science and The Graduate University for Advanced Studies) for useful discussion. When I encountered difficulties, he helped me, and supported my studies. The present author would also thank Prof. Roberto D Rivarola (Instituto Fisica de Rosario) and Dr. Pablo Fainstein (Centro Atomico Bariloche) for helpful discussion, advice and supports.

The present author wishes to acknowledge Prof. Victor Ponce (Centro Atomico Bariloche), Prof. Toshiaki Kaneko (Okayama Univ. for Science), Dr. Kazumoto Hosaka, Mr. Takahiro Kenmotsu, Mr. Masaki Nishiura (Graduate Univ. for Adv. Studies), Dr. Toshiki Takahashi (Gumma Univ.), Mr. Daiyu Hayashi(Nagoya Univ.), Dr. Kengo Moribayashi (Japan Atomic Energy Research Institute) and the members of Instituto Fisica de Rosario, Argentina, for useful discussion.